Arabian Journal of Chemistry (2021) **14**, 103304

King Saud University

Arabian Journal of Chemistry

www.ksu.edu.sa
www.sciencedirect.com

ORIGINAL ARTICLE

Synthesis, characterization, docking study and biological evaluation of new chalcone, pyrazoline, and pyrimidine derivatives as potent antimalarial compounds

Mohammad Murwih Alidmat [a], Melati Khairuddean [a,*], Naziera Mohammad Norman [a], Anis Nasihah Mohamed Asri [a], Mohd Hisyam Mohd Suhaimi [a], Garima Sharma [b]

[a] *School of Chemical Sciences, University Sains Malaysia, 11800 Penang, Malaysia*
[b] *Faculty of Science, Motherhood University, Roorkee-Dehradun Road Bhagwanpur, Karaundi, Uttarakhand 247661, India*

Received 11 May 2021; accepted 30 June 2021
Available online 6 July 2021

KEYWORDS

Chalcone;
Pyrazoline;
Pyrimidine;
Malaria

Abstract Malaria is a protozoan disease caused by a unicellular parasite named *Plasmodium* (Phylum- Apicomplexa). World Health Organization has estimated roughly fifty percent of the world's community lives under the continuing threat of malaria. The focus of drug discovery has increased towards valuable structures known as chalcones, pyrazoline, and pyrimidine due to their extensive bioactivity in malaria treatment. In this study, four chalcone derivatives (**1**–**4**) have been synthesized via the Claisen-Schmidt condensation. New compounds of 12 pyrazolines **(1**–**4)Ai-iii** and eight pyrimidines, **(1**–**4)Bi-ii** derivatives have also been synthesized via a ring-closing reaction of the chalcones. All the synthesized compounds were characterized and tested against malaria. The results showed that compound **1Aiii** exhibited significant antiproliferative effects against 3D7 and RKL9 with 3D7 = 2.1 μg/mL, IC_{80} 3D7 = 8 μg/mL, and IC_{50} RKL9 when exposed to compared to the reference anticancer drug, CQ Chloroquine diphosphate, and Artemisinin. The molecular docking analysis showed that compounds 1, 1Aiii and 1Bi had entered the PfATP4 receptor pocket and had been stuck with the amino acids in a high affinity of binding.

* Corresponding author.
E-mail address: melati@usm.my (M. Khairuddean).
Peer review under responsibility of King Saud University.

Production and hosting by Elsevier

1. Introduction

Malaria is caused by the Plasmodium parasite, which is transmitted by the bite of a mosquito vector. Malaria is among the most devastating and widespread tropical parasitic diseases in developing countries. According to the

https://doi.org/10.1016/j.arabjc.2021.103304
1878-5352 Published by Elsevier B.V. on behalf of King Saud University.

World Health Organization (WHO), it was estimated at around 229 million malaria cases in 2019 in 87 malaria-endemic countries. In general, about fifty percent of the world's community lives under the continuing threat of malaria (Organization, 2020). Five species of plasmodium commonly known to infect humans are P. falciparum, Plasmodium vivax, Plasmodium ovalae, Plasmodium malariae, and Plasmodium knowelsi. However, parasite P. falciparum causes the highest rates of complications and mortality (Shibeshi et al., 2020). The parasites enter the human body via the bite of an infected mosquito which, enters the bloodstream, multiply in the liver cells before released back into the bloodstream, where they quickly rearrange by inserting their proteins, infecting and destroy the red blood cells. The malaria parasite life cycle involves two hosts. During a blood meal, a malaria-infected female Anopheles mosquito inoculates sporozoites into the human host. Sporozoites infect liver cells and mature into schizonts , which rupture and release merozoites (Baer et al., 2007).

The intraerythrocytic malaria parasite, Plasmodium falciparum, maintains a low cytosolic Na(+) concentration and the plasma membrane P-type cation translocating ATPase 'PfATP4′ has been implicated as playing a key role in this process. PfATP4 has been the subject of significant attention in recent years as mutations in this protein confer resistance to a growing number of new antimalarial compounds, including the spiroindolones, the pyrazoles, the dihydroisoquinolones, and a number of the antimalarial agents in the Medicines for Malaria Venture's 'Malaria Box'. On exposure of parasites to these compounds there is a rapid disruption of cytosolic Na(+)(Spillman et al., 2013). Whether, and if so how, such chemically distinct compounds interact with PfATP4, and how such interactions lead to parasite death, is not yet clear. The fact that multiple different chemical classes have converged upon PfATP4 highlights its significance as a potential target for new generation antimalarial agents(Spillman and Kirk, 2015). A spiroindolone (KAE609, now known as cipargamin) has progressed through Phase I and IIa clinical trials with favourable results. In this review we consider the physiological role of PfATP4, summarise the current repertoire of antimalarial compounds for which PfATP4 is implicated in their mechanism of action, and provide an outlook on translation from target identification in the laboratory to patient treatment in the field(Bouwman et al., 2020).

Malaria is a global problem and the lack of a credible malaria vaccine and the emergence and spread of parasites resistant to most of the clinically used antimalarial drugs and drug combinations have aroused an imperative need to develop new drugs against malaria. Antimalarial drug resistance is the ability of a parasite strain to survive and/or to multiply despite the administration of medicine given in doses equal to or higher than those usually recommended. Antimalarial drug resistance is a major threat to malaria control in which the widespread and indiscriminate use of antimalarial drugs such as chloroquine and artemisinin contributes to malaria parasites to evolve the mechanisms of resistance (Cheo et al., 2020; Haston et al., 2019). Therefore, it is important to design new antimalarial agents for effective therapy. Since natural products are more biological-friendly, antimalarial agents with natural product scaffold have been explored in the development of target compounds. Many small molecule drugs in the market were developed from natural-based scaffolds which can be considered as privileged structures for the discovery of new antimalarials (Jampilek, 2017; Tajuddeen and Van Heerden, 2019; Wells, 2011). Nevertheless, some difficulties associated with the natural lead compounds derived from these scaffolds, such as their synthesis, limited aqueous solubility, chemical or metabolic instability, and a wide spectrum of biological effects need to be overcome. These antimalarial agents will continue to be in demand for the complete management of malaria and the issue of resistance (Jampilek, 2017; Sinha et al., 2013).

Chalcone is a simple structure that has been widely used as an effective template in drug discovery. As an important group of the secondary metabolites of the flavonoid family, compounds with chalcone scaffold (Fig. 1) have been reported to exhibit a variety of biological activities for various infectious diseases including malaria(Hameed et al., 2019; Qin et al., 2020; Sinha et al., 2019; Tajuddeen et al., 2018; Thillainayagam et al., 2015). Chalcone derivatives with substituents such as prenyl, allyl, alkoxy and hydroxyl groups have been reported to exhibit good antimalarial activity. Such substituents have the potential to increase the lipophilicity of a compound which is an important property in antimalarial activity (Prashar et al., 2012; Tadigoppula et al., 2013; Yadav et al., 2012). Furthermore, the enone group in chalcone, located in between the phenyl rings play important role in antimalarial activity because it binds better to the active site of the parasite (Batagin-Neto and Lavarda, 2014; Insuasty et al., 2015; Syahri et al., 2017).

Since the huge demand for chalcone compounds cannot be fulfilled from natural sources, these compounds can be synthesized. Chalcone is a well-known precursor for the synthesis of various heterocyclic compounds. Cyclization of chalcone leads to heterocyclic compounds bearing nitrogen-containing rings such as pyrazoline and pyrimidine (Fig. 1) with potential antimalarial activity (Insuasty et al., 2013; Nehra et al., 2020). Pyrazoline is among the most prominent five-membered heterocyclic ring containing two adjacent nitrogen atoms (Fig. 1); one is pyrrole-like nitrogen which is non-basic nitrogen with a lone pair involved in the aromaticity while the other is pyridine-like nitrogen with a lone pair on an sp^2 orbital which is basic and nucleophilic(Bennani et al., 2020). Pyrazoline has only one endocyclic double bond in which 2-pyrazoline is the most common derivatives (Gupta et al., 2018). Pyrimidine, on the other hand, is a 6-membered heterocyclic ring containing two nitrogen atoms at positions 1 and 3. Pyrimidine and its derivatives have gained prominence because of their potential pharmaceutical values (Jain et al., 2016; Wang et al., 2016; Ye et al., 2015).

This research work focused on the synthesis of some potential compounds with chalcone, pyrazoline and pyrimidine scaffolds. Chalcone compounds, **1 – 4** were synthesized via the Claisen-Schmidt condensation. The cyclization reaction of these chalcones formed a series of pyrazoline and pyrimidine derivatives, accordingly. Meanwhile, in vitro antimalarial activity assay was conducted between the synthesized compounds against Plasmodium falciparum 3D7 strain. The best compound was further investigated using the molecular docking technique to understand the compound activity.

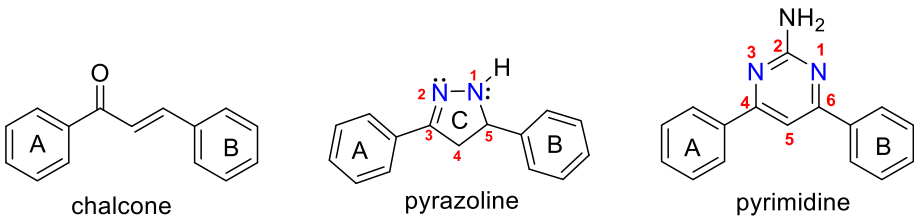

Fig. 1 Structures of chalcone, pyrazoline and pyrimidine.

2. Result and discussion

2.1. Anti-Malaria activity of the synthesized compounds

All the synthesized compounds were evaluated for their antimalarial activity against RKL9 (a chloroquine-resistant strain) of *P. falciparum* and 3D7 (chloroquine-sensitive) reference strains which were used as control. The IC_{50} and IC_{80} values of the compounds obtained were compared with two references (Chloroquine diphosphate, CQ, and Artemisinin). All these results are summarized in Table 1.

All compounds **(1–4, $1A_{i\text{-}iii}$-$4A_{i\text{-}iii}$, $1B_{i\text{-}ii}$ – $4B_{i\text{-}ii}$)** prepared in this study were tested for their antimalarial activity against *P. falciparum*, in which most of the compounds showed good activity compared to the references. Among all the tested compound, **1Aiii** was found to be the most active with IC_{50} 3D7 = 2.1 μg/mL, IC_{80} 3D7 = 8 μg/mL, and IC_{50}RKL9 = 1.1 μg/mL (Table 1). The presence of carbothioamide functionality affects the activity of compounds **2Aiii**, **3Aiii**, and **4Aiii.** Chalcones **1, 2, 3** and **4** have shown less antimalarial activity against *P. falciparum* compared to the heterocyclic compounds derived from these chalcones. Moreover, compounds bearing a methoxy group in the *para* position showed better activity than the compounds bearing a methoxy group in the *meta* position as shown in Fig. 2**.**

2.2. Molecular docking

The behavior of all synthesized compounds was studied. To be an effective drug, a compound must have optimum hydrophilic and hydrophobic properties to be transported in blood before penetrating the cell membrane(Cama et al., 2019). Water solubility depends on the number of hydrogen bond donors relative to the compound's alkyl side chain. Low water solubility means slow absorption and bioavailability. Too many hydrogen bond donors contribute to low-lipophilicity, leading to

Table 1 Antimalarial activity against *P. falciparum* (μg/mL).

Compound	IC_{50} 3D7 μg/mL	IC_{80} 3D7 μg/mL	IC_{50} RKL9 μg/mL	Resistance Index (IC_{50} 3D7/IC_{50} RKL9)
CQ Chloroquine diphosphate	20.63	36.11	206.37	0.1
Artemisinin	4.51	8.46	4.51	1.0
1	8.4	19	4.2	2.0
2	5.2	24	4.1	1.2
3	22.2	24	6.4	3.5
4	14.1	23	6.5	3.2
1Ai	6.2	15	2.2	2.8
1Aii	4.2	9	3.4	1.2
1Aiii	2.1	8	1.1	1.9
1Bi	6.3	14	2.9	2.1
1Bii	9.9	19.7	6.1	1.6
2Ai	2.1	15	4.3	0.48
2Aii	4.9	14	3.6	1.3
2Aiii	1.3	12	2.1	0.61
2Bi	5.4	16	2.4	2.2
2Bii	4.2	9	2.2	1.7
3Ai	18.2	16	7.3	2.4
3Aii	16.2	15.2	5.5	2.9
3Aiii	7.6	14.4	3.4	2.2
3Bi	20	42	10.5	1.9
3Bii	12.2	34.2	5.4	2.2
4Ai	3.2	11	2.9	1.1
4Aii	6.2	14	2.9	2.1
4Aiii	2.2	6	1.1	2.0
4Bi	4.4	10	3.2	1.3
4Bii	5.1	12	2.0	2.5

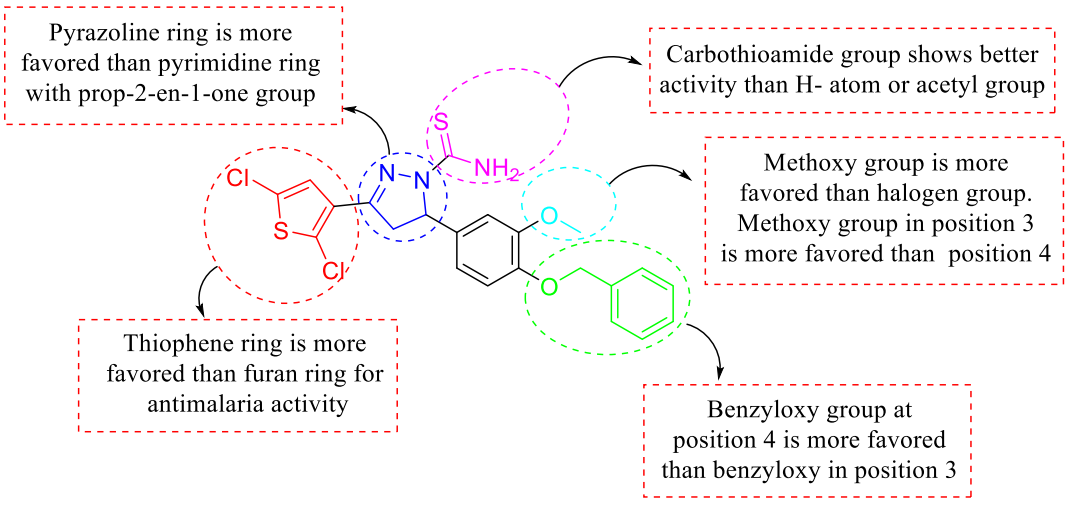

Fig. 2 The results obtained from different structure compounds model.

the drug's inability to cross the cell membrane(Stewart et al., 2017). A simple method to evaluate the drug-like properties is to check the compliance with Lipinski's rule (rule of 5), which specifies the numbers of hydrophilic groups, molecular weight, and hydrophobicity. Lipinski's rule of five theorize that an active oral drug should have (i) not more than five hydrogen bond donors (OH and NH groups); (ii) not more than five hydrogen bond acceptors (notably N and O); (iii) molecular weight less than 500 g/mol; and (iv) octanol–water partition coefficient (log P) less than 5 (Zhang and Wilkinson, 2007), as shown in Table 2. Moreover, Table 2 displays the computed scores of docking between The PfATP4 receptor structure (receptor) and all the synthesized compounds (ligands). The more negative value shows a high probability of interaction between the ligand and the receptor. As expected, all the compound derivatives that entered the PfATP4 pocket possessed varying scores with the enclosed amino acids.

In Table 2, all the compounds tested showed a good affinity to the active site of PfATP4 with free binding energy ranging

Table 2 Chemical properties based on Lipinski's rule (rule of 5), free binding energy (FBE) with the inhibition constant (Ki) of all compounds derivatives.

Compound	MW	Binding Energy Kcal/mol	Ki, nM	H-Bond	Log P
1	419.32	− 9.64	105.05	3	5.78
1Ai	433.35	−10.16	101.03	2	5.05
1Aii	475.38	−9.53	104.43	2	5.05
1Aiii	492.43	−11.05	86.04	3	5.23
1 Bi	458.36	−10.35	98.05	2	6.16
1 Bii	475.40	−10.08	102.03	2	7.14
2	419.32	−9.43	106.05	2	5.78
2Ai	433.35	−9.42	111.00	3	5.05
2Aii	475.38	−9.87	143.94	3	5.05
2Aiii	492.43	−10.03	143.03	2	5.23
2 Bi	458.36	−8.56	157.09	2	6.16
2 Bii	475.40	−8.64	187.03	2	7.14
3	334.37	−8.59	145.03	2	3.68
3Ai	348.40	−8.21	132.07	3	2.99
3Aii	390.44	−8.43	111.03	3	2.94
3Aiii	407.49	−9.05	106.08	3	3.17
3 Bi	373.41	−9.07	114,0.90	2	4.10
3 Bii	390.46	−9.67	119.06	2	5.09
4	334.37	−9.01	132.09	2	3.68
4Ai	348.40	−9.72	130.32	3	2.99
4Aii	390.44	−8.64	123.02	3	2.94
4Aiii	407.49	−8.63	120.30	2	3.17
4Bi	373.41	−9.03	112.32	2	4.10
4Bii	390.46	−9.05	113.01	2	5.09

from –11.05 to –8.56 kcal/mol. Remarkably, compounds **1, 1Aiii,** and **1Bi** displayed free binding energy of – 9.64, −11.05 and-10.35 kcal/mol, respectively. Few series of chalcone, pyrazoline, and pyrimidine derivatives have been designed with various thiophene, furan, and methoxyphenyl scaffolds attached at both ends. The results have shown that the aromatic ring in compounds **1**, **1Aiii,** and **1Bi** formed hydrophobic interactions in the binding site of 2DQS.PDB (Figs. 3–5). The docking results of compound **1** (chalcone) formed two π-σ bond with ILE 235, and PRO 681 and also three hydrogen bonds with ASN 201, ASN201, and ARG 489. The thiol group in compound **1** formed one π-lone pair bond with the thiol group of VAL 679. The docking of compound **1** was also found to form two π-alkyl, alkyl bonds with ARG 678 and VAL 200, and three hydrogen bonds with ASN 201, VAL 679, and GLU 680. Compound **1** also formed one carbon-hydrogen bond with LEU 180. On the other hand, the docking results of compound **1Aiii** formed two π-cation bonds with ARG 489 and three hydrogen bonds with ASN 201, VAL 679, and GLU 680. The thiol group in compound **1Aiii** (pyrazoline) formed one hydrogen bond with the thiol group of ASN 201. The docking of compound **1Aiii** was also found to form one van der Waals with GLU 680, and four alkyls, π- alkyl bonds with ILE 235, PRO 681, VAL 200 and LEU 180. Finally, the docking results of compound **1Bi** (pyrimidine) formed two π-cation and π-anion bonds with LYS 684 and two with ASP 351, and two hydrogen bonds with ASP 703, and ASP 707. The thiol group in compound **1Bi** formed one sulfur-X bond with the thiol group of THR 353. The docking of compound **1Bi** was also found to form one van der Waals with GLU 680, three alkyls, π- alkyl bonds with VAL 200, LYS 352 and PRO 681, and one carbon-hydrogen bond with VAL 679.

All these bondings improved and stabilized the interaction within the active site for a long time, which is essential and needed to inhibit the activity of 2DQS. Compound **1Aiii** was found to exhibit the hydrogen bond interaction with the ASN 201 in the PfATP4 active site, which explained their cytotoxic activity *in vitro* assay.

3. Conclusion

A series of four chalcones (**1**–**4**) were successfully synthesized between 4-benzyloxy-3-methoxybenzaldehyde or 3-ben zyloxy-4-methoxybenzaldehyde of 3-acetyl-2,5-dichlorothiophene (**1**–**2**) and 2-acetylfuran (**3**–**4**), separately. These chalcones, **1**–**4** were used for further *cyclo*-condensation reactions with hydrazine hydrate derivatives to form twelve new pyrazoline derivatives, **(1–4)A(i-iii).** The reaction of these chalcones with guanidine or thiourea formed eight new pyrimidine derivatives, **(1–4)B(i-ii).** All the compounds were characterized using FT-IR, ^{1}H and ^{13}C NMR spectroscopy. The cytotoxic activity of all the synthesized compounds was evaluated against malaria. The presence of carbothioamide functionality has shown good activity of pyrazoline compounds **(1–4)Aiii** with pyrazoline **1Aiii** to be the most active (IC_{50} 3D7 = 2.1, IC_{80} 3D7 = 8, and IC_{50}RKL9 = 1.1). All chalcones **1**–**4** have shown less antimalarial activity against *P. falciparum* compared to the heterocyclic compounds derived from these chalcones. Moreover, compounds bearing a methoxy group in the *para* position showed better activity than a methoxy group in the *meta* position**.** The molecular docking analysis showed that a compound with a larger structure has an increasing number of bonds, leading to more interactions with the residues of amino acids in the active PfATP4 site, which could have enhanced the antimalaria activity. Furthermore, the docking scores showed that the binding energies of the synthesized compounds 1, 1Aiii and 1Bi to the PfATP4 receptor were the best of all the synthesized derivatives.

4. Materials and methods

4.1. Materials

Reagents and solvents used were purchased as analytical grade and used without further purification unless stated otherwise.

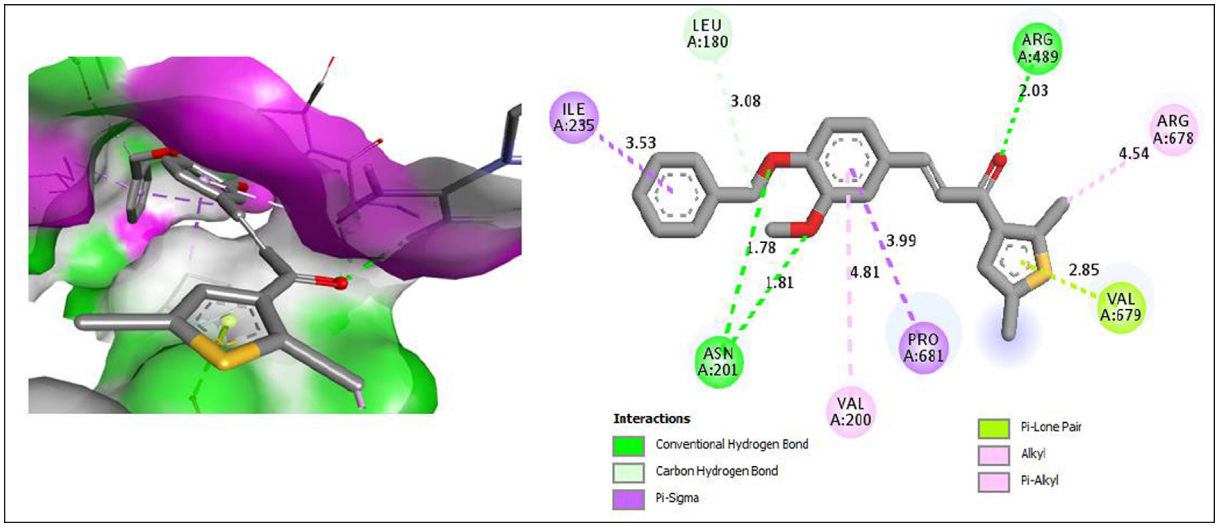

Fig. 3 The best predicted binding poses of (a) 2D- and (b) 3D-molecular structure interaction of compounds **1** with 2DQS.PDB. In the scaffold, green color represents the carbon atoms, red for oxygen, sky blue for fluorine, dark blue for chlorine, and pale blue for the nitrogen atom.

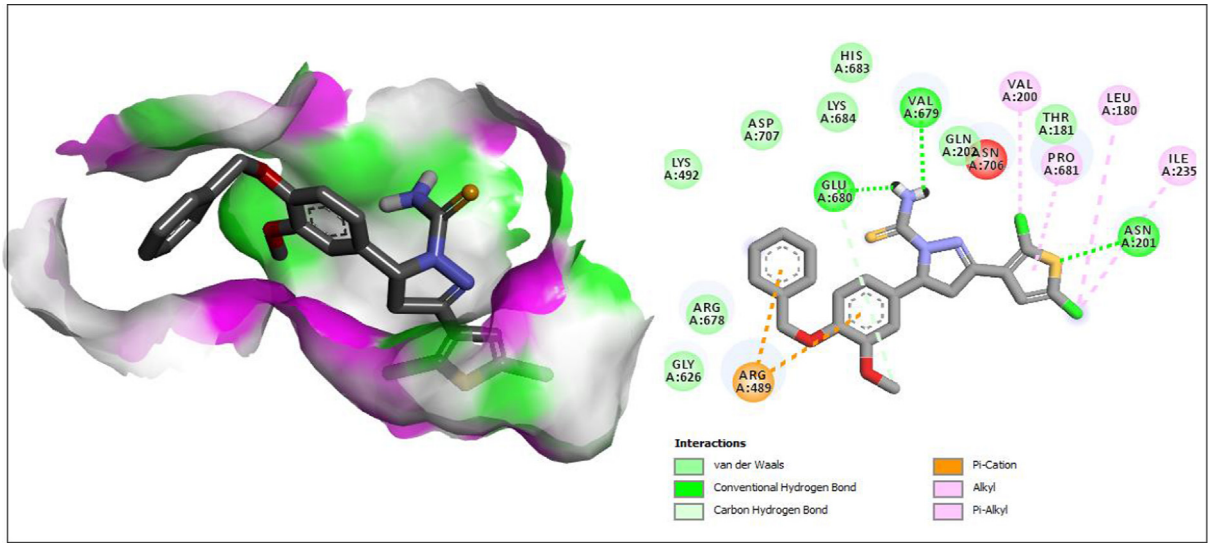

Fig. 4 The best predicted binding poses of (a) 2D- and (b) 3D-molecular structure interaction of compounds **1Aiii** with 2DQS.PDB. In the scaffold, green color represents the carbon atoms, red for oxygen, sky blue for fluorine, dark blue for chlorine, and pale blue for the nitrogen atom.

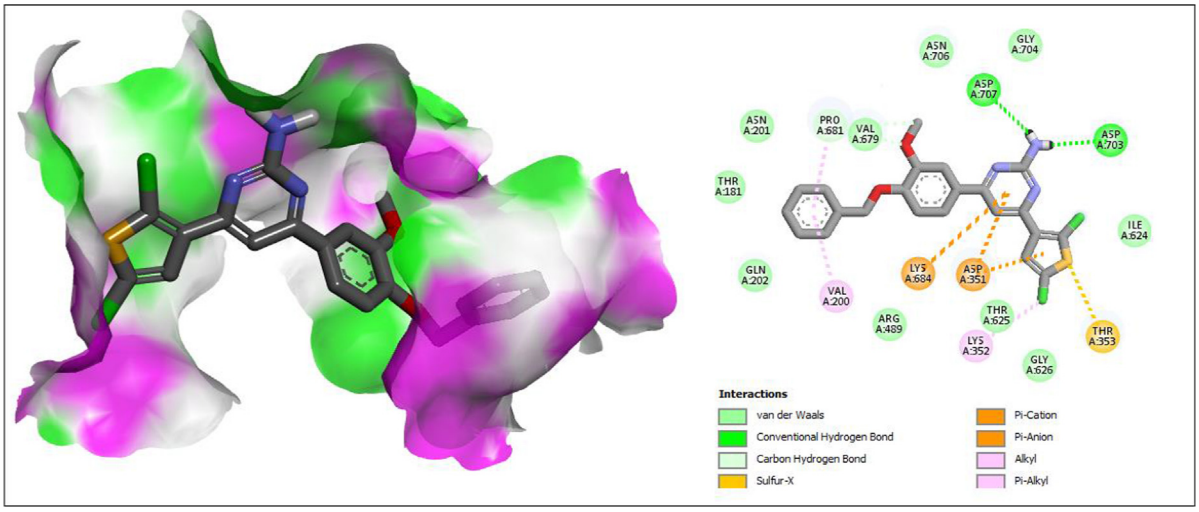

Fig. 5 The best predicted binding poses of (a) 2D- and (b) 3D-molecular structure interaction of compound **1Bi** with 2DQS.PDB. In the scaffold, green color represents the carbon atoms, red for oxygen, sky blue for fluorine, dark blue for chlorine, and pale blue for the nitrogen atom.

Thin Layer Chromatography (TLC) paper silica gel and Kieselguhr coated with Flourescent indicator F254 was used to monitor the reaction progress and visualization of spots was done under UV light machine. Melting points were determined with the Melting point (Stuart SMP10) apparatus and are uncorrected. The NMR spectra were recorded using Bruker-Advance 500 MHz Ultrashield^{TM} spectrometer. DMSO d_6 or $CDCl_3$ were used as the solvent with tetramethylsilane as the internal reference. Chemical shifts (δ) are quoted relative to TMS. Unequivocal ^{13}C assignments were made based on experiments. Attenuated Total Reflection (ATR) Nicolet 6700 FT-IR spectrometer with the frequency range of 600–4000 cm^{-1} was used to determine the absorption bands of the functional groups.

4.2. Synthesis methods

4.2.1. Synthesis of chalcone derivatives, 1–4 (Ibrahim et al., 2012; Salum et al., 2020)

The reaction involves the Claisen-Schmidt condensation (Scheme 1) between 0.01 mol of 3-acetyl-2,5-dichlorothiophene or 2-acetylfuran (0.01 mol) and 4-benzyloxy-3-methoxybenzaldehyde or 3-benzyloxy-4-methoxybenzaldehyde with (0.01 mol) in 25.0 mL of ethanol in the presence of NaOH as a catalyst. The reaction mixture was stirred at room temperature for 6–24 h. The reaction progress was monitored by TLC. The precipitate formed was filtered, washed with cold water, and dried to give a yellow solid. The solid product was recrystallized from methanol to give a yellow powder.

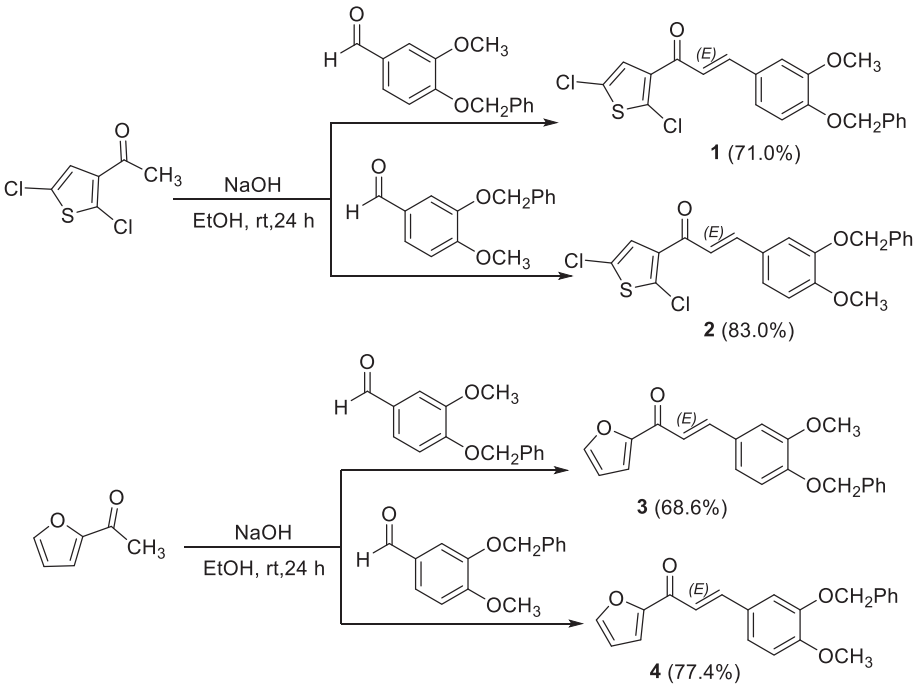

Scheme 1 Synthesis of chalcones **1**–**4.**

*4.2.1.1. 3-(4-(benzyloxy)-3-methoxyphenyl)-1-(2,5-dichlorothiophen-3-yl)prop-2-en-1-one, **1**.*

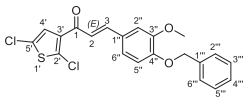

Yield: 71.0%. Color: yellow solid. M.p.:118–123 °C, MW: 419.32. FT-IR (cm^{-1}): 3032 (Csp^2-H str.), 2881 (Csp^3-H str.), 1644 (C = O str.), 1510 (C = C str.), 989 (C-O str.), 694 (C-Cl str.). ^{1}H NMR (500 MHz, $CDCl_3$) δ, ppm: 3.97 (s, CH_3, 3H), 5.24 (s, CH_2, 2H), 6.92 (d, J = 8.5 Hz, H-3, 1H), 7.16 (t, J = 3.0 Hz, H-2‴, H-6‴, 2H), 7.18 (d, J = 2.0 Hz, H-5″, 1H), 7.20 (s, H-2″, 2H), 7.24 (s, H-4′, 1H), 7.35 (d, J = 7.5 Hz, H-6″, 1H), 7.41 (t, J = 7.0 Hz, H-4‴, 1H), 7.46 (d, J = 7.5 Hz, H-3‴, H-5‴, 2H), 7.70 (d, J = 15.5 Hz, H-2, 1H). ^{13}C NMR (125 MHz, $CDCl_3$) δ, ppm: 56.1 (CH_3), 70.8 (CH_2), 110.8 (C-2″), 113.4 (C-5″), 121.8 (C-2), 123.2 (C-6″), 126.9 (C-3′), 127.1 (C-5′), 127.2 (C-4′), 127.7 (C-2‴, 6‴), 128.1 (C-1″), 128.7 (C-4‴), 130.6 (C-3‴, 5‴), 136.4 (C-1‴), 138.0 (C-2′), 145.7 (C-3), 149.8 (C-4″), 150.9 (C-3″), 184.0 (C-1). CHN elemental analysis: Calculated for $C_{21}H_{16}Cl_2O_3S$: C: 60.15%, H: 3.85%. Found: C: 59.85%, H: 3.55%.

*4.2.1.2. (E)-3-(3-(benzyloxy)-4-methoxyphenyl)-1-(2,5-dichlorothiophen-3-yl)prop-2-en-1-one, **2**.*

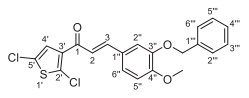

Yield: 83%. Color: yellow solid; mp: 175–180 °C. MW: 419.32. IR (ν, cm^{-1}): 3102 and 3028 (C^2_{sp}-H str.); 2923 and 2833 (C^3_{sp}-H str.), 1643 (C = O str.), 1571 (C = C aromatic atr.), 1506 (C = C alkenyl str.), 1137 (C-O), 1007 (C-S), 812 (C-Cl). ^{1}H NMR (500 MHz, $CDCl_3$) δ, ppm: 3.96 (s, CH_3, 3H), 5.23 (s, CH_2, 2H), 6.93 (d, J = 10.0 Hz, H-2, 1H), 7.12–7.49 (m, H-aromatic, 9H), 7.65 (d, J = 15.5 Hz, H-3, 1H). ^{13}C NMR (125 MHz, $CDCl_3$) δ, ppm: 56.0 (CH_3), 71.2 (CH_2), 111.5 (C-5′), 112.9 (C-2″), 121.5 (C-2), 124.0 (C-6″), 126.8 (C-3″), 127.2 (C-5′), 127.2 (C-4′), 127.3 (C-1″), 128.1 (C-2‴,6‴), 128.7 (C-4‴), 130.7 (C-3‴,5‴), 136.7 (C-1‴), 138.0 (C-2′), 145.5 (C-3), 148.3 (C-4″), 152.4 (C-3″), 183.8 (C-1). CHN Elemental analysis for $C_{21}H_{16}Cl_2O_3S$: Calculated: C, 60.15%; H, 3.85%; Found: C, 59.80%; H, 3.55%.

*4.2.1.3. (E)-3-(4-benzyloxy)-3-methoxyphenyl)-1-(furan-2-yl) prp-2-en-1-one, **3**.*

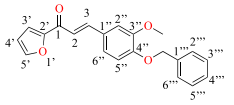

Yield: 68.6%. Color: Yellow solid. Melting point: 117–122 °C. FT-IR (ATR, cm^{-1}): 3022–3115 (C-H $^2_{sp}$), 2847–2980 (C-H $^3_{sp}$), 1653 (C = C str.), 1583 and 1509 (C = C str.), 1009 (C-O str.) ^{1}H NMR (500 MHz, $CDCl_3$) δ, ppm: 3.94 (s, CH_3, 3H), 5.21 (s, CH_2, 2H), 6.67 (dd, J = 1.5 Hz, 5.0 Hz, 1H), 6.92 (d, J = 8.5 Hz, 1H), 7.21 (d, J = 9 Hz, 1H), 7.26 (dd, J = 3 Hz, J = 7.5 Hz, 1H), 7.29 (d, J = 3.5 Hz, 1H), 7.34 (d, J = 7.5 Hz, 1H), 7.40 (t, J = 15 Hz, 2H), 7.48 (d, J = 7.5 Hz, 2H), 7.65 (s, 1H), 7.77 (s, 1H). ^{13}C NMR (125 MHz, $CDCl_3$) δ, ppm: 56.1 (CH_3), 71.3 (CH_2), 111.6 (C-2″), 112.5 (C-4′), 113.3 (C-5″), 117.1 (C-3′), 119.1 (C-2),

123.6 (C-6′′), 127.5 (C-2′′′, C-6′′′), 127.7 (C-1′), 128.1 (C-4′′′), 128.7 (C-3′′′, C-5′′′), 136.7 (C-1′′′), 144.0 (C-3), 146.3 (C-4′′), 148.4 (C-5′), 152.2 (C-3′′), 153.9 (C-2′), 178.1 (C-1). Analytical calcd for $C_{21}H_{18}O_4$ (%): C: 75.43%; H: 5.43%. Found: C: 75.12%; H: 5.13%.

4.2.1.4. (E)-3-(3-(benzyloxy)-4-methoxyphenyl)-1-(furan-2-yl) prop-2-en-1-one, ***4****.*

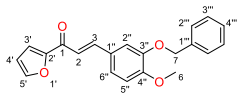

Yield: 77.4%. Color: yellow powder, m.p: 135–140 °C, FT-IR (cm^{-1}): 3118 (Csp^2-H stretching), 2944 and 2847 (Csp^3-H stretching), 1653 (C = O stretching), 1583C = C stretching), 1509 (aromatic C = C stretching), 1259 (aromatic C-O stretching) and 1007 (C-O stretching). ^{1}H NMR (500 MHz, $CDCl_3$) δ, ppm: 3.97 (s, 3H, C-6), 5.22 (s, 2H, C-7), 6.59 (dd, 1H, *J* = 1.5, 3.5 Hz, H-4′), 6.91 (d, 1H, *J* = 9.0 Hz, H-3), 7.15 (d, 1H, *J* = 7.5 Hz, H-2′′), 7.30–7.45 (m, 7H, H-3′,5′,5′′,6′′,2′′′,3′′′,4′′′), 7.65 (d, 1H, *J* = 1.0 Hz, H-5′), 7.83 (d, 1H, *J* = 15.5 Hz, H-2). ^{13}C NMR (125 MHz, $CDCl_3$) δ, ppm: 56.1 (C-6), 70.8 (C-7), 110.8 (C-5′′), 112.5 (C-4′), 113.4 (C-2′′), 117.1 (C-3′), 119.1 (C-2), 123.1 (C-6′′), 123.2 (C-2′′′), 128.0 (C-1′′), 128.1 (C-4′′′), 128.6 (C-3′′′), 136.5 (C-1′′′), 144.1 (C-3), 146.2 (C-5′), 149.7 (C-4′′), 150.6 (C-3′′), 153.8 (C-2′), 178.1 (C-1). CHN elemental analysis: Calculated for $C_{21}H_{18}O_4$: C: 75.43%, H: 5.43%; Found C: 75.18%, H: 5.15%.

4.2.2. Synthesis of pyrazoline compounds, (1–4)Ai-iii (Salum et al., 2020)

Cyclization of chalcone precursors with a series of hydrazine derivatives in ethanol or acetic acid gave pyrazoline compounds. A mixture of chalcone, **1 – 4** (0.02 mol) with hydrazine hydrate (0.02 mol) in 15.0 mL of ethanol was stirred at room temperature for 24 h. The reaction progress was monitored by TLC. The precipitate formed was filtered off, washed with cold water, and dried. The solid product was recrystallized from ethanol (see Scheme 2) (Ibrahim, 2015).

4.2.2.1. 5-(4-(benzyloxy)-3-methoxyphenyl)-3-(2,5-dichlorothiophen-3-yl)-4,5-dihydro-1H-pyrazole, ***1Ai****.*

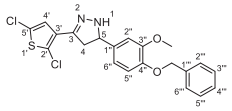

Yield: 66.2%. Color: white powder. M.p.: 131–136 °C, MW: 433.35. FT-IR (cm^{-1}): 3355 (N-H stretching), 3025 (Csp^2-H str.), 2904 (Csp^3-H str.), 1594 (C = N ctr.), 1513 (C = C str.), 1130 (C-N STR.), 1009 (C-O STR.), 690 (C-Cl). ^{1}H NMR (500 MHz, $CDCl_3$) δ, ppm: 3.35 (dd, J_{H4a-5} = 3.63 Hz, J_{H4a-b} = 15.13 Hz, H-4a, 1H), 3.35 (dd, J_{H5-4a} = 12.5 Hz, J_{H5-H4b} = 18.0 Hz, H-5, 1H), 3.93 (s, CH_3, 3H), 5.17 (s, CH_2, 2H), 5.55 (dd, J_{H4b-5} = 3.62, J_{H4b-a} = 15.12 Hz, H-4b, 1H), 6.09 (s, NH, 1H), 6.72 (d, *J* = 8.0 Hz, H-5′′, 1H), 6.81 (s, H-4′, 1H), 6.87 (d, *J* = 8.0 Hz, H-6′′, 1H), 7.32 (s, H-2′′, 1H), 7.35 (d, *J* = 7.0 Hz, H-6′′′, 1H), 7.41 (t, *J* = 6.5 Hz, H-3′′′,5′′′,4′′′, 2H), 7.47 (d, *J* = 6.5 Hz, H-2′′′, 2H). ^{13}C NMR (125 MHz, $CDCl_3$) δ, ppm: 44.8 (C-4), 57.2 (C-5), 61.0 (CH_3), 72.1 (CH_2), 110.7 (C-2′′), 115.2 (C-5′′), 118.5 (C-3′), 126.8 (C-6′′), 127.9 (C-5′), 128.2 (C-2′′′, 6′′′), 128.5 (C-4′′′), 128.9 (C-2′), 129.6 (C-4′), 130.9 (C-3′′′, 5′′′), 135.7 (C-1′′′), 138.2 (C-1′′), 148.8 (C-4′′), 149.5 (C-3′′), 150.9 (C-3). CHN elemental analysis: Calculated for $C_{21}H_{18}Cl_2N_2O_2S$: C: 58.21%, H: 4.19%, N: 6.46%. Found: C:57.89%, H: 3.87%, N:6.16%.

4.2.2.2. 5-(3-(benzyloxy)-4-methoxyphenyl)-3-(2,5-dichlorothiophen-3-yl)-4,5-dihydro-1H-pyrazole, ***2Ai****.*

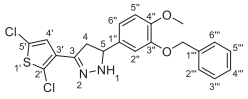

Yield: 75.0%. Color: white powder. M.p.: 136–141 °C, MW: 433.35. FT-IR (cm^{-1}): 3355 (N-H stretching), 3025 (Csp^2-H str.), 2900 (Csp^3-H str.), 1560(C = N ctr.), 1513 (C = C str.), 1130 (C-N STR.), 1007 (C-O STR.), 696 (C-Cl). ^{1}H NMR (500 MHz, $CDCl_3$) δ, ppm: 3.35 (dd, J_{H4a-5} = 4 Hz, J_{H4a-b} = 16.0 Hz, H-4a, 1H), 4.35 (dd, J_{H5-4a} = 4 Hz, J_{H5-H4b} = 16.0 Hz, H-5, 1H), 3.93 (s, CH_3, 3H), 5.17 (s, CH_2, 2H), 5.64(dd, J_{H4b-5} = 5, J_{H4b-a} = 15.12 Hz, H-4b, 1H), 6.07 (s, NH, 1H), 6.72 (d, *J* = 8.0 Hz, H-5′′, 1H), 6.81 (s, H-4′, 1H), 6.87 (d, *J* = 8.0 Hz, H-6′′, 1H), 7.32 (s, H-2′′, 1H), 7.35 (d, *J* = 7.0 Hz, H-6′′′, 1H), 7.41 (t, *J* = 6.5 Hz, H-3′′′,5′′′,4′′′, 2H), 7.47 (d, *J* = 6.5 Hz, H-2′′′, 2H). ^{13}C NMR (125 MHz, $CDCl_3$) δ, ppm: 44.8 (C-4), 57.2 (C-5), 61.0 (CH_3), 72.1 (CH_2), 110.7 (C-2′′), 115.2 (C-5′′), 118.5 (C-3′), 126.8 (C-6′′), 127.9 (C-5′), 128.2 (C-2′′′, 6′′′), 128.5 (C-4′′′), 128.9 (C-2′), 129.6 (C-4′), 130.9 (C-3′′′, 5′′′), 135.7 (C-1′′′), 138.2 (C-1′′), 148.8 (C-4′′), 149.5 (C-3′′), 150.9 (C-3). CHN elemental analysis: Calculated for $C_{21}H_{18}Cl_2N_2O_2S$: C: 58.23%, H: 4.19%, N: 6.46%. Found: C:57.89%, H: 3.90%, N:6.18%.

4.2.2.3. 5-(4-(benzyloxy)-3-methoxyphenyl)-3-(furan-2-yl)-4,5-hydro-1H-pyrazole, ***3Ai****.*

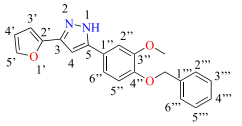

Yield: 20.92%. Color: Brown solid. Melting point: 156–161 °C. FT-IR (ATR, cm^{-1}): 3039–3061 (C-H sp^2 str.), 2885–2983 (C-H sp^3 str.), 1650.7 (C = N str.), 1550–1640 (C = C str.), 1009.1 (C-O str.) ^{1}H NMR (500 MHz, $CDCl_3$) δ, ppm: 2.37 (dd, *J* = 4.5 Hz, 17.5 Hz, 1H), 3.10 (dd, *J* = 4.5 Hz, 17.5 Hz, 1H) 3.69 (dd, *J* = 12.0 Hz, 17.5 Hz, 1H), 3.94 (s, CH_3, 3H), 5.21 (s, CH_2, 2H), 6.60 (dd, *J* = 1.5 Hz, 3.5 Hz, 1H), 6.92 (d, *J* = 8.5 Hz, 1H), 7.21 (d, *J* = 9.0 Hz, 1H), 7.25–7.49 (m, 8H). ^{13}C NMR (125 MHz,

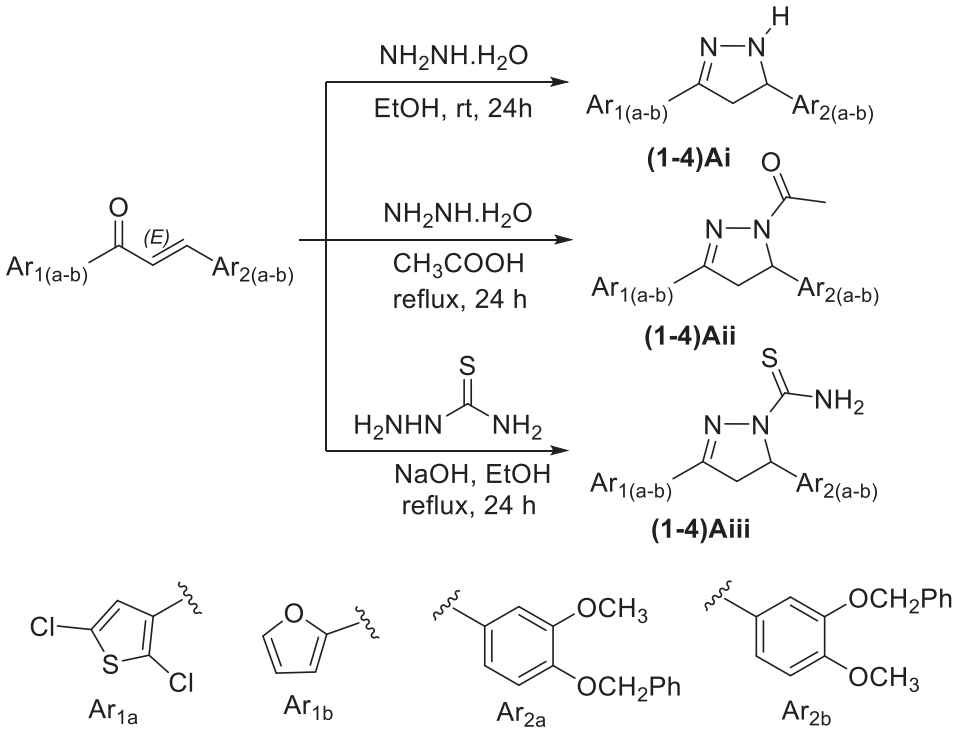

Scheme 2 Synthesis of pyrazoline derivatives **(1–4)A(i-iii)**.

$CDCl_3$) δ, ppm: 40.2 (C-4), 49.0 (C-5), 57.0 (CH3), 72.2 (CH2), 112.6 (C-3′), 113.5 (2′′), 114.3 (C-4′), 118.1 (C-5′′), 120.0 (C-6′′), 124.6 (C-2′′′, C-6′′′), 128.4 (C-4′′′), 128.6 (C-3′′′, C-5′′′), 129.1 (C-1′′′), 129.6 (C-1′′), 137.7 (C-5′), 145.0 (C-2′), 147.3 (C-4′′), 149.3 (C-3′′), 154.8 (C-3). Analytical calcd for $C_{21}H_{19}O_3N_2$ (%): C: 74.10%; H: 5.33%; N: 4.12%. Found: C: 73.78%; H: 5.02%; N: 4.42%

4.2.2.4. (E)-3-(3-(benzyloxy)-4-methoxyphenyl)-1-(furan-2-yl) prop-2-en-1-one, ***4Ai****.*

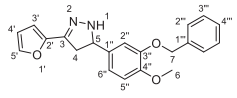

Yield: 52.77%. Color: brown powder, m.p: 123–128 °C, FT-IR (cm-1): 3150 and 3117 (N-H stretching), 3038 (Csp^2-H stretching), 2982 and 2945 (Csp^3-H stretching), 1651 (C = N stretching), 1587 (C = C stretching), 1263 (C-N stretching), 1086 (aromatic C-O stretching), and 1041 (C-O stretching). ^{1}H NMR (500 MHz, $CDCl_3$) δ, ppm: 2.99 (dd, 1H, *J* = 5.0, 7.0 Hz, H-4a), 3.82 (s, 2H, H-6), 4.19 (dd, 1H, *J* = 1.0, 2.0 Hz, H-5), 5.18 (s, 2H, H-7), 5.43 (dd, 1H, *J* = 2.0, 4.0 Hz, H-4b), 6.80 (dd, 1H, *J* = 2.0 4.0 Hz, H-4′), 6.165 (s, 1H, N-H), 7.36 (d, 1H, *J* = 7.5 Hz, H-3′), 7.39–7.78 (m, 6H, H-2′′,5′′,6′′,2′′′,3′′′,4′′′), 7.61 (d, 1H, *J* = 2.0 Hz, H-5′). ^{13}C NMR (125 MHz, $CDCl_3$) δ, ppm: 41.2 (C-4), 56.1 (C-5), 63.7 (C-6), 70.9 (C-7), 111.4 (C-3′), 111.7 (C-2′′), 111.9 (C-4′), 119.1 (C-6′′), 127.4 (C-5′′), 127.5 (C-2′′′), 127.5 (C-4′′′), 127.8 (C-3′′′), 128.5 (C-1′′′), 128.5 (C-1′′), 136.8 (C-5′), 143.4 (C-2′), 148.2 (C-4′′), 148.3 (C-3′′), 149.3 (C-3). CHN elemental analysis: Calculated for $C_{21}H_{20}N_2O_3$: C: 72.40%, H: 5.79, N: 8.04%; Found: C: 72.12%, H: 5.52%, N: 8.22%.

4.2.2.5. 1-(5-(4-(benzyloxy)-3-methoxyphenyl)-3-(2,5-dichlorothiophen-3yl)-4,5-dihydro-1H-pyrazol-1-yl)ethan-1-one, ***1Aii****.*

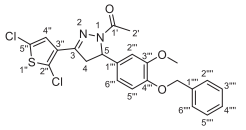

Yield: 44.1%. Color: white powder. M.p.: 133–139 °C, MW: 475.38. FT-IR (cm^{-1}): 3029 (Csp^2-H str.), 2908 (Csp^3-H str.), 1668 (C = N str.), 1513 (C = O str,), 1130 (C-N str.), 1013 (C-O str.), 694 (C-Cl str.). ^{1}H NMR (500 MHz, $CDCl_3$) δ, ppm: 2.39 (s, H-2′, 3H), 3.32 (d, *J* = 18.0 Hz, H-4a, 1H), 3.83 (dd, $J_{H5\text{-}a}$ = 12.5 Hz, $J_{H5\text{-}b}$ = 18.0 Hz, H-5, 1H), 3.90 (s, CH_3, 3H), 5.14 (s, CH_2, 2H), 5.51 (d,

J = 18.0 Hz, H-4b,1H), 6.68 (d, J = 8.0 Hz, H-5‴,1H), 6.78 (s, H-4′, 1H), 6.83 (d, J = 8.0 Hz, H-6‴, 1H), 7.29–7.44 (m, H-2‴, 2‴,3‴, 4‴, 5‴, 6‴, 6H). ^{13}C NMR (125 MHz, $CDCl_3$) δ, ppm: 21.9 (C-2′), 43.7 (C-4), 56.1 (CH_3), 60.0 (C-5), 71.0 (CH_2), 109.6 (C-2‴), 114.1 (C-5″), 117.4 (C-3″), 125.7 (C-6‴), 126.9 (C-5‴), 127.2 (2‴, 6‴), 127.4 (C-4‴), 127.8 (C-4″), 128.5 (C-3‴, 5‴), 129.8 (C-2″), 137.1 (C-1‴), 147.8 (C-4‴), 148.4 (C-3‴), 149.8 (C-3), 168.9 (C-1′). CHN elemental analysis: Calculated for $C_{23}H_{20}Cl_2N_2O_3S$: C: 58.11%, H: 4.24%, N: 5.89%. Found: C: 57.80%, H: 4.02%, N: 6.11%.

4.2.2.6. 1-(5-(3-(benzyloxy)-4-methoxyphenyl)-3-(2,5-dichlorothiophen-3yl)-4,5-dihydro-1H-pyrazol-1-yl)ethan-1-one, ***2Aii****.*

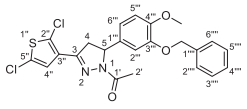

Yield: 76%. Color: white powder. M.p.: 135–140 °C, MW: 480.48. FT-IR (cm^{-1}): 3029 (Csp^2-H str.), 2910 (Csp^3-H str.), 1670 (C = N str.), 1520 (C = O str,), 1135 (C-N str.), 1015 (C-O str.), 702 (C-Cl str.). ^{1}H NMR (500 MHz, $CDCl_3$) δ, ppm: 2.45 (s, H-2′, 3H), 3.38 (d, J = 18.5 Hz, H-4a, 1H), 3.73 (dd, $J_{H5\text{-}a}$ = 12.5 Hz, $J_{H5\text{-}b}$ = 18.0 Hz, H-5, 1H), 3.95 (s, CH_3, 3H), 5.09 (s, CH_2, 2H), 5.48 (d, J = 18.0 Hz, H-4b,1H), 6.67 (d, J = 8.0 Hz, H-5‴,1H), 6.88 (s, H-4′, 1H), 6.93 (d, J = 8.0 Hz, H-6‴, 1H), 7.25–7.44 (m, H-2‴, 2‴,3‴, 4‴, 5‴, 6‴, 6H). ^{13}C NMR (125 MHz, $CDCl_3$) δ, ppm: 23.9 (C-2′), 45.7 (C-4), 57.1 (CH_3), 60.0 (C-5), 73.0 (CH_2), 110.6 (C-2‴), 115.1 (C-5″), 117.4 (C-3″), 125.2 (C-6‴), 126.4 (C-5‴), 127.2 (2‴, 6‴), 127.4 (C-4‴), 127.8 (C-4″), 128.5 (C-3‴, 5‴), 130.8 (C-2″), 138.1 (C-1‴), 147.4 (C-4‴), 148.2 (C-3‴), 149.5 (C-3), 169.9 (C-1′). CHN elemental analysis: Calculated for $C_{23}H_{20}Cl_2N_2O_3S$: C: 58.11%, H: 4.24%, N: 5.89%. Found: C: 57.83%, H: 4.04%, N: 6.12%.

4.2.2.7. 1-(5-(4-(benzyloxy)-3-(methoxyphenyl)-3-(furan-2-yl)4,5-dihydro-1H-pyrazole-1-yl)ethan-1-one, ***3Aii****.*

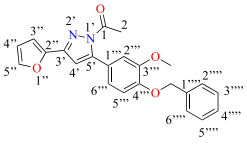

Yield: 64.10%. Color: Brown solid. Melting point: 100–105 °C. FT-IR (ATR, cm^{-1}): 3033–3129 (C-H $^2_{sp}$ str.), 2940–2977 (C-H $^3_{sp}$ str.), 1697 (C = O str.), 1654 (C = N str.), 1000 (C-O str.), ^{1}H NMR (500 MHz, $CDCl_3$) δ, ppm: 2.08 (s, 1H), 3.10 (dd, J = 4.5 Hz, J = 4.5 Hz, 1H), 3.69 (dd, J = 12 Hz, 1H), 3.88 (s, CH_3, 3H), 5.13 (s, CH_2, 2H), 5.53 (dd, J = 4.25 Hz, J = 11.75 Hz, 1H), 6.74 (d, J = 3.5 Hz, 1H), 6.79 (d, J = 2 Hz, 1H), 6.83 (d, J = 8.5 Hz, 1H), 7.28–7.58 (m, 8H). ^{13}C NMR (125 MHz, $CDCl_3$) δ, ppm: 22.0 (CH_3), 42.1 (C-4′), 56.1 (CH3), 59.3 (5′), 71.0 (CH2), 109.6 (C-3′), 112.0 (C-2‴), 112.2 (C-4″), 117.5 (C-5‴), 127.2 (C-6‴), 127.8 (C-2‴,C-6‴), 128.6 (C-4‴), 134.7 (C-3‴,C-5‴), 137.1 (C-1‴), 144.8 (C-1‴), 145.7 (C-5″), 146.9 (C-2″), 147.8 (C-4‴), 149.9 (C-3‴), 169.0 (C-1). Analytical calcd for $C_{23}H_{22}O_4N_2$ (%): C: 71.12%; H: 5.16%; N: 7.21%. Found: C: 70.77%; H: 4.80%; N: 7.53%.

4.2.2.8. (5-(3-(benzyloxy)-4-methoxyphenyl)-3-(furan-2-yl)-4,5-dihydro-1H-pyrazol-1-yl) ethan-1-one, ***4Aii****.*

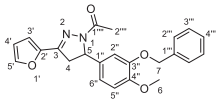

Yield: 39.55%. Color: orange yellow powder, m.p: 135–140 °C. FT-IR (cm^{-1}): 3062 (Csp^2-H stretching), 2968 and 2870 (Csp^3-H stretching), 1651 (C = O stretching), 1601 (C = N stretching), 1517 (a C = C stretching), 1251 (C-N stretching), 1133 (C-O stretching), and 1009 (C-O stretching). ^{1}H NMR (500 MHz, $CDCl_3$) δ, ppm: 2.39 (s, 3H, H-2‴), 2.99 (dd, 1H, J = 4.0, 17.5 Hz, H-4a), 3.63 (dd, 1H, J = 12.0, 17.5 Hz, H-5), 3.86 (s, 3H, H-6), 5.12 (s, 2H, H-7), 5.47 (dd, 1H, J = 4.0, 11.5 Hz, H-4b), 6.55–7.60 (m, 9H, H-3′,4′5′,2″,5″,6″,2‴,3‴,4‴). ^{13}C NMR (125 MHz, $CDCl_3$) δ, ppm: 22.0 (C-2‴), 41.9 (C-4), 56.0 (C-6), 59.1 (C-5), 71.1 (C-7), 111.6 (C-3′), 111.9 (C-2″), 111.9 (C-4′), 112.7 (C-6″), 118.6 (C-5″), 127.5 (C-2‴), 127.8 (C-4‴), 128.5 (C-3‴), 134.0 (C-1″), 136.9 (C-1‴), 144.7 (C-5′), 145.6 (C-2′), 146.8 (C-4″), 148.4 (C-3″), 149.2 (C-3), 168.8 (C-1‴). CHN elemental analysis: Calculated for $C_{23}H_{22}N_2O_4$: C: 70.75%, H: 5.68%, N: 7.18%; Found C: 70.47%, H: 5.55%, N: 7.38%.

4.2.2.9. 5-(4-(benzyloxy)-3-methoxyphenyl)-3-(2,5-dichlorothiophen-3-yl)-4,5-dihydro-1H-pyrazole-1-carbothioamide, ***1Aiii****.*

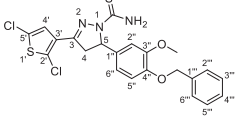

Yield: 62.2%. Color: brown powder. M.p.: 83–88 °C, MW: 492.43. FT-IR (cm^{-1}): 3449 (N-H str.), 3271 (N-H str.), 3143 (Csp^2-H str.), 2931 (Csp^3-H str.), 1574 (C = N str.), 1137 (C-N str.), 1026 (C-O str.), 828 (C = S str.), 694 (C-Cl str.). ^{1}H NMR (500 MHz, $CDCl_3$) δ, ppm: 3.29 (dd, $J_{4a\text{-}5}$ = 2.0 Hz, $J_{4a\text{-}b}$ = 15.5 Hz, H-4a, 1H), 3.80 (dd, $J_{5\text{-}4a}$ = 12.5 Hz, $J_{H5\text{-}4b}$ = 18.0 Hz, H-5, 1H), 4.37 (s, NH, 1H), 5.11 (s, CH_2, 2H), 5.48 (dd, $J_{4b\text{-}5}$ = 2.0 Hz, $J_{4b\text{-}a}$ = 15.5 Hz, H-4a, 1H), 6.66 (d, J = 8.0 Hz, H-5″, 1H), 6.75 (s, H-4′, 1H), 6.80 (d, J = 8.5 Hz, H-6″, 2H), 7.26–7.39 (m, H-2″, 2‴, 3‴, 4‴, 5‴, 6‴, 6H), 8.40 (s, NH, 1H). ^{13}C NMR (125 MHz, $CDCl_3$) δ, ppm: 44.5 (C-4), 56.9 (CH_3), 60.8 (CH_2), 71.8 (C-5), 110.5 (C-5″), 115.0 (C-3′), 118.2 (C-6″), 126.5 (C-5′), 128.0 (C-2‴, 6‴), 128.3 (C-4‴), 128.6 (C-2′), 129.4 (C-3‴, 5‴), 130.6 (C-4′), 135.5 (C-1″), 137.9 (C-1‴), 148.6 (C-4″), 149.3 (C-3″), 150.6 (C-3), 178.7 (C = S). CHN

elemental analysis: Calculated for $C_{22}H_{19}Cl_2N_3O_2S_2$: C: 53.66%, H: 3.89%, N: 8.53%. Found: C: 53.38%, H: 3.60%, N: 8.83%.

4.2.2.10. 5-(3-(benzyloxy)-4-methoxyphenyl)-3-(2,5-dichlorothiophen-3-yl)-4,5-dihydro-1H-pyrazole-1-carbothioamide, ***2Aiii****.*

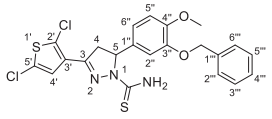

Yield: 75%. Color: brown powder. M.p.: 120–125 °C, MW: 492.43 FT-IR (cm^{-1}): 3460 (N-H str.), 3275 (N-H str.), 3145 (Csp^2-H str.), 2939 (Csp^3-H str.), 1590 (C = N str.), 1159 (C-N str.), 1054 (C-O str.), 825 (C = S str.), 690 (C-Cl str.). ^{1}H NMR (500 MHz, $CDCl_3$) δ, ppm: 3.5 (dd, $J_{4a\text{-}5}$ = 2.5 Hz, $J_{4a\text{-}b}$ = 15.5 Hz, H-4a, 1H), 3.75 (dd, $J_{5\text{-}4a}$ = 12.0 Hz, $J_{H5\text{-}4b}$ = 16.5 Hz, H-5, 1H), 4.37 (s, NH, 1H), 5.30 (s, CH_2, 2H), 5.60 (dd, $J_{4b\text{-}5}$ = 2.5 Hz, $J_{4b\text{-}a}$ = 16.0 Hz, H-4a, 1H), 6.68 (d, *J* = 8.5 Hz, H-5′′, 1H), 6.65 (s, H-4′, 1H), 6.87 (d, *J* = 8.5 Hz, H-6′′, 2H), 7.24–7.42 (m, H-2′′, 2′′′, 3′′′, 4′′′, 5′′′, 6′′′, 6H), 8.46 (s, NH, 1H). ^{13}C NMR (125 MHz, $CDCl_3$) δ, ppm: 44.8 (C-4), 56.0 (CH_3), 63.8 (CH_2), 75.8 (C-5), 112.5 (C-5′′), 114.7 (C-3′), 115.2 (C-6′′), 126.0 (C-5′), 128.6 (C-2′′′, 6′′′), 128.9 (C-4′′′), 128.9 (C-2′), 129.0 (C-3′′′, 5′′′), 131.6 (C-4′), 134.5 (C-1′′), 138.7 (C-1′′′), 149.0 (C-4′′), 150.3 (C-3′′), 152.6 (C-3), 179.9 (C = S). CHN elemental analysis: Calculated for $C_{22}H_{19}Cl_2N_3O_2S_2$: C: 53.66%, H: 3.89%, N: 8.53%. Found: C: 53.37%, H: 3.57%, N: 8.88%.

4.2.2.11. 5-(4-(benzyloxy)-3-methoxyphenyl)-3-(furan-2-yl)-4,5-dihydro-1H-pyrazole-1-carbothioamide, ***3Aiii****.*

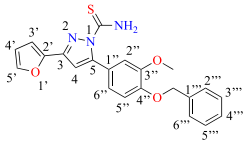

Yield: 50.49%. Color: light yellow solid. Melting point: 101–106 °C. FT-IR (ATR, cm^{-1}): 3500–3600 (N-H str.), 2838–2859 (C-H sp^3 str.), 1260 (C-O), 800–805 (C = S) Yield: Brown solid. Melting point: 101–102 °C. ^{1}H NMR (500 MHz, $CDCl_3$) δ, ppm: 3.03 (dd, *J* = 3.25 Hz, *J* = 17.8 Hz, 1H), 3.72 (dd, *J* = 11.5 Hz, *J* = 17.5 Hz, 1H), 3.87 (s, 1H, NH), 5.18 (d, *J* = 41 Hz, 2H), 5.91 (dd, *J* = 3.25 Hz, *J* = 11.25 Hz, 1H), 7.26–7.61 (m, 8H), 9.84 (s, NH, 1H). ^{13}C NMR (125 MHz, $CDCl_3$) δ, ppm: 42.7 (C-4), 56.0 (CH_3), 62.7 (C-5), 71.2 (CH2), 111.8 (C-3′), 111.9 (C-2′), 112.3 (C-4′), 114.1 (C-5′′), 118.5 (C-6′′), 127.5 (C-2′′′,C-6′′′), 127.5 (C-4′′′), 127.7 (C-3′′′, C-5′′′), 128.5 (C-1′′), 137.0 (C-1′′′), 145.4 (C-5′), 146.2 (C-2′), 148.3 (C-4′′), 153.8 (C-3′′), 157.3 (C-3), 168.5 (C = S). Analytical calcd for $C_{22}H_{21}O_3N_3$ (%): C: 65.17%; H: 4.72%; N: 10.36%. Found: C: 64.81%; H: 4.36%; N: 10.06%.

4.2.2.12. 5-(3-(benzyloxy)-4-methoxyphenyl)-3-(furan-2-yl)-4,5-dihydro-1H-pyrazole-1-carbothioamide, ***4Aiii****.*

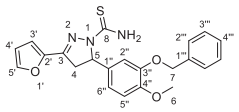

Yield: 41.83%. Color: brown powder, m.p: 180–185 °C, FT-IR (cm-1): 3445 and 3333 (N-H stretching), 3131 (Csp^2-H stretching), 2934 and 2877 (asymmetrical and symmetrical Csp^3-H), 1670 (C = N stretching), 1582 (aromatic C = C stretching), 1320 (NCS stretching), 1256 (C-N stretching), 1133 (aromatic C-O stretching), and 1014 (C-O stretching). ^{1}H NMR (500 MHz, $CDCl_3$) δ, ppm: 3.03 (d, 1H, *J* = 14.0 Hz, H-6a), 3.71 (dd, 1H, *J* = 11.5, 17.5 Hz, H-1), 3.93 (s, 3H, H-6), 5.19 (s, 2H, H-7), 5.92 (d, 1H, *J* = 9.5 Hz, H-4b), 6.57 (s, 2H, NH_2), 6.75–7.61 (m, 8H, H-3′,4′,5′,2′′,5′′,6′′,4′′′, 5′′′,6′′′). ^{13}C NMR (125 MHz, $CDCl_3$) δ, ppm: 42.0 (C-4), 55.9 (C-6), 62.6 (C-5), 71.1 (C-7), 111.7 (C-3′), 111.8 (C-2′′), 112.3 (C-4′), 114.0 (C-6′′), 118.4 (C-5′′), 127.7 (C-2′′′), 128.4 (C-4′′′), 128.6 (C-3′′′), 133.9 (C-1′′), 136.9 (C-1′′′), 145.3 (C-5′), 146.2 (C-2′), 147.2 (C-4′′), 148.3 (C-3′′), 149.2 (C-3), 176.5 (C-8). CHN elemental analysis: Calculated for $C_{22}H_{21}N_3O_3S$: C: 64.85%, H: 5.19%, N: 10.31%; Found C: 64.58% , H: 4.89% , N: 10.17%.

4.2.3. Synthesis of the pyrimidine compounds (Alidmat, 2015)

The preparation of pyrimidine compounds involves the reaction of chalcone **1** to **4** (1 mol) with guanidine or thiourea (1 mol) separately, as shown in Scheme 3. Chalcone **1Bi** is used as a representative. A mixture of chalcone (1 mol), guanidine (1 mol), NaOH (1 mol), and 15.0 mL ethanol was refluxed for 24 h. The reaction progress was monitored by TLC. The precipitate formed was filtered off, washed with cold water, and dried. The solid product was recrystallized from ethanol (Nisa and Yusuf, 2020).

4.2.3.1. 4-(4-(benzyloxy)-3-methoxyphenyl)-3-(2,5-dichlorothiophen-3-yl) pyrimidin-2-amine, ***1Bi****.*

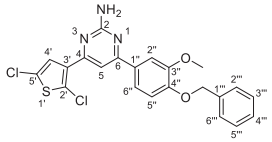

Yield: 42.1%. Color: brown powder. M.p.: 130–135 °C, MW: 458.36. FT-IR (cm^{-1}): 3361 (N-H str.), 3062 (Csp^2-H str.), 2935 (Csp^3-H str.), 1571 (C = N str.), 1134 (C-N str.), 1006 (C-O str.), 697 (C-Cl str.). ^{1}H NMR (500 MHz, DMSO d_6) δ, ppm: 3.87 (s, CH_3, 3H), 5.18 (s, CH_2, 2H), 6.77 (s, NH_2, 2H), 7.17 (d, *J* = 8.5 Hz, H-5′′, 2H), 7.36 (d, *J* = 7.0 Hz, H-6′′,1H), 7.41 (t, *J* = 7.0 Hz, H-4′′′, 2H), 7.47 (s, H-2′′, 1H), 7.56 (s, H-4′, 1H), 7.70 (d, *J* = 8.5 Hz, H-5′′′ 0.6′′′. 2H), 7.73 (s, H-2′′′, 3′′′, 2H). ^{13}C NMR (125 MHz, DMSO d_6) δ, ppm: 56.1 (CH_3), 70.3 (CH_2), 104.1 (C-5),

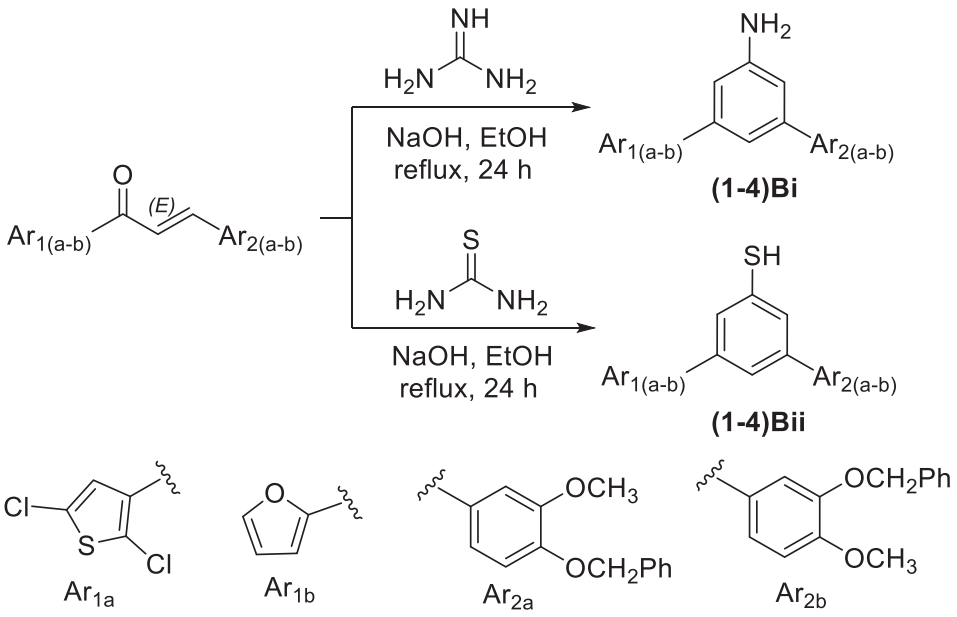

1: Ar_{1a}, Ar_{2a}; **2**: Ar1a, Ar_{2b}; **3**: Ar_{1b}, Ar_{2a}; **4**: Ar_{1b}, Ar_{2b}

Scheme 3 Synthesis of pyrimidine derivatives **(1–4)B(i-ii)**.

110.6 (C-2′′), 113.5 (C-5′′), 120.5 (C-4′), 125.5 (C-6′′), 128.3 (C-2′), 128.4 (C-2′′′, 6′′′), 128.5 (C-4′′′), 128.9 (C-3′′′, 5′′′), 130.2 (C-1′′), 136.9 (C-5′), 137.2 (C-1′′′), 149.5 (C-3′), 150.6 (C-3′′, 4′′), 159.5 (C-4), 164.1 (C-2), 165.1 (C-6). CHN elemental analysis: Calculated for $C_{22}H_{17}Cl_2N_3O_2S$: C: 57.65%, H: 3.74%, N: 9.17%. Found: C: 57.33%, H: 3.43%, N: 8.85%.

4.2.3.2. 4-(4-(benzyloxy)-3-methoxyphenyl)-6-(2,5-dichlorothiophen-3-yl) pyrimidine-2-thiol, ***1Bii***.

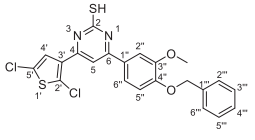

Yield: 82.8%. Color: brown powder. M.p: 84–89 °C, MW: 475.40. FT-IR (cm^{-1}): 3063 (Csp^2-H str.), 2977 (Csp^3-H str.), 2877 (S-H str.), 1653 (C = N str.), 1136 (C-N str.), 1007 (C-O str.), 696 (C-Cl str.). ^{1}H NMR (500 MHz, DMSO) δ, ppm: 1.57 (s, SH, 1H), 3.91 (s, CH_3, 3H), 5.18 (s, CH_2, 2H), 7.12 (dd, J = 2.3 Hz, J = 10.8 Hz, H-5′′,6′′, 2H), 7.18 (s, H-4′, 1H), 7.23 (s, H-2′′, 1H), 7.29 (t, J = 7.0 Hz, H-2′′′,6′′′, 1H), 7.35 (t, J = 7.5 Hz, H-4′′′, 2H), 7.41 (d, J = 7.5 Hz, H-3′′′, 5′′′, 2H). ^{13}C NMR (125 MHz, DMSO) δ, ppm: 56.6 (CH_3), 70.8 (CH_2), 111.1 (C-2′′), 114.0 (C-5), 121.0 (C-5′′), 126.1 (C-4′), 128.8 (C-6′′), 128.8 (C-2′), 128.9 (C-4′′′), 129.0 (C-3′), 129.4 (C-2′′′, 6′′′), 130.7 (C-1′′′), 137.4 (C-5′′′), 137.7 (C-3′′′), 150.0 (C-1′′), 151.1 (C-5′), 160.0 (C-4), 164.6 (C-6), 178.8 (C-2). CHN elemental analysis: Calculated for $C_{22}H_{16}Cl_2N_2O_2S_2$: C: 55.58%, H: 3.39%, N: 5.89%. Found: C: 55.28%, H: 3.09%, N: 5.54%.

4.2.3.3. 4-(3-(benzyloxy)-4-methoxyphenyl)-3-(2,5-dichlorothiophen-3-yl)pyrimidin-2-amine, ***2Bi***.

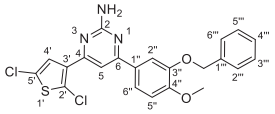

Yield: 42.1%. Color: brown powder. M.p.: 135–140 °C, MW: 458.36. FT-IR (cm^{-1}): 3361 (N-H str.), 3062 (Csp^2-H str.), 2935 (Csp^3-H str.), 1571 (C = N str.), 1134 (C-N str.), 1008 (C-O str.), 700 (C-Cl str.). ^{1}H NMR (500 MHz, DMSO d_6) δ, ppm: 3.87 (s, CH_3, 3H), 5.20 (s, CH_2, 2H), 6.87 (s, NH_2, 2H), 7.19 (d, J = 8.5 Hz, H-5′′, 2H), 7.36 (d, J = 7.0 Hz, H-6′′,1H), 7.45 (t, J = 7.5 Hz, H-4′′′, 2H), 7.49 (s, H-2′′, 1H), 7.56 (s, H-4′, 1H), 7.72 (d, J = 8.0 Hz, H-5′′′ 0.6′′′. 2H), 7.76 (s, H-2′′′, 3′′′, 2H). ^{13}C NMR (125 MHz, DMSO d_6) δ, ppm: 56.1 (CH_3), 70.3 (CH_2), 105.1 (C-5), 111.6 (C-2′′), 112.5 (C-5′′), 121.5 (C-4′), 126.5 (C-6′′), 127.3 (C-2′), 127.4 (C-2′′′, 6′′′), 127.5 (C-4′′′), 128.9 (C-3′′′, 5′′′), 131.2 (C-1′′), 136.9 (C-5′), 136.2 (C-1′′′), 148.5 (C-3′), 151.6 (C-3′′, 4′′), 158.5 (C-4), 165.1 (C-2), 165.4 (C-6). CHN elemental analysis: Calculated for $C_{22}H_{17}Cl_2N_3O_2S$: C: 57.65%, H: 3.74%, N: 9.17%. Found: C: 57.35%, H: 3.40%, N: 8.86%.

4.2.3.4. 4-(3-(benzyloxy)-4-methoxyphenyl)-6-(2,5-dichlorothiophen-3-yl) pyrimidine-2-thiol, ***2Bii***.

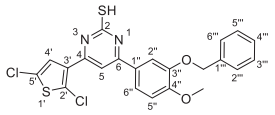

Yield: 82.8%. Color: brown powder. M.p: 184–190 °C, MW: 475.40. FT-IR (cm^{-1}): 3067 (Csp^2-H str.), 2987 (Csp^3-H str.), 2897 (S-H str.), 1658 (C = N str.), 1130 (C-N str.), 1003 (C-O str.), 692 (C-Cl str.). ^1H NMR (500 MHz, DMSO) δ, ppm: 1.62 (s, SH, 1H), 3.68 (s, CH_3, 3H), 5.56 (s, CH_2, 2H), 7.6 (dd, J = 3 Hz, J = 10.7 Hz, H-5'',6'', 2H), 7.16 (s, H-4′, 1H), 7.27 (s, H-2'', 1H), 7.24 (t, J = 7.3 Hz, H-2''',6''', 1H), 7.37 (t, J = 7.8 Hz, H-4''', 2H), 7.45 (d, J = 7.3 Hz, H-3''', 5''', 2H). ^{13}C NMR (125 MHz, DMSO) δ, ppm: 56.8 (CH_3), 70.9 (CH_2), 111.1 (C-2''), 114.9 (C-5), 121.7 (C-5''), 126.7 (C-4′), 128.9 (C-6''), 128.2 (C-2′), 128.4 (C-4'''), 129.7 (C-3′), 129.9 (C-2''', 6'''), 131.9 (C-1'''), 135.4 (C-5'''), 138.7 (C-3'''), 152.0 (C-1''), 153.1 (C-5′), 161.0 (C-4), 164.6 (C-6), 179.8 (C-2). CHN elemental analysis: Calculated for $C_{22}H_{16}Cl_2N_2O_2S_2$: C: 55.54%, H: 3.39%, N: 5.89%. Found: C: 55.24%, H: 3.07%, N: 5.55%.

4.2.3.5. 4-(4-(benzyloxy)-3-methoxyphenyl)-6-(furan-2-yl) pyrimidin-2-amine, ***3Bi****.*

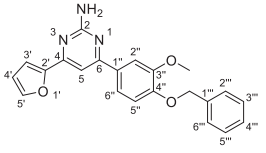

Yield: 53.11%. Light brown solid. Melting point: 192–197 °C. FTIR (ATR, cm^{-1}): 3117–3132 (N-H str.), 3033–3061 (C-H sp^2 str.), 2840–2980 (C-H sp^3 str.), 1651 (C = N str.), ^1H NMR (500 MHz, $CDCl_3$) δ, ppm: 3.77 (s, CH_3, 3H), 5.06 (s, CH_2, 2H), 6.59 (s, NH_2, 2H), 7.07 (d, J = 8 Hz, 1H), 7.17–7.38 (m, 8H), 7.62 (d, J = 9.5 Hz, 2H), 7.80 (s, 1H). ^{13}C NMR (125 MHz, $CDCl_3$) δ, ppm: 56.1 (CH_3), 70.3 (CH_2), 99.8 (C-5), 110.6 (C-3′), 112.0 (C-2''), 112.9 (C-5''), 113.5 (C-4′), 120.4 (C-6''), 128.2 (C-2''', C-6'''), 128.4 (C-4'''), 128.43 (C-2''', C-5'''), 128.9 (C-1''), 130.3 (C-1'''), 137.3 (C-5′), 145.6 (C-4''), 149.5 (C-5''), 150.5 (C-2′), 152.6 (C-N), 156.7 (C-4), 164.1 (C-6). Analytical calcd for $C_{22}H_{19}O_3N_3$ (%): C: 70.76%; H: 5.13%; N: 11.25%. Found: C: 70.40%; H: 4.77%; N: 10.94%.

4.2.3.6. 4-(4-(benzyloxy)-3-methoxyphenyl)-6-(furan-2-yl) pyrimidine-2-thiol, ***3Bii****.*

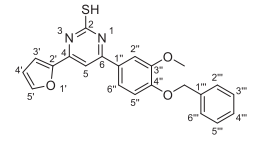

Yield: 87.09%. Color: dark brown solid. Melting point: 152–157 °C. FT-IR (ATR, cm^{-1}): 3033 and 3100 (C-H sp^2 str.), 2847 and 2937 (C-H sp^3 str.), 2550 and 2620 (S-H, weak), 1650 (C = N str.), 1600 (C = C str.), 1003 (C-O str.). ^1H NMR (500 MHz, $CDCl_3$) δ, ppm: 3.06 (s, SH), 3.77 (s, CH_3, 3H), 5.06 (s, CH_2, 2H), 7.07 (d, J = 8 Hz, 1H), 7.17 (s, 1H), 7.23–7.38 (m, 9H), 7.61 (d, J = 5 Hz, 1H), 7.80 (s, 1H). ^{13}C NMR (125 MHz, $CDCl_3$) δ, ppm: 56.2 (CH_3), 71.0 (CH_2), 98.2 (C-5), 106.8 (C-3′), 110.5 (C-2''), 111.8 (C-5''), 114.0 (C-4′), 119.3 (C-6''), 127.2 (C-2''', C-6'''), 127.3 (C-4'''), 128.0 (C-3''', C-5'''), 128.56 (C-1''), 128.62 (C-1'''), 135.0 (C-5′), 136.8 (C-4''), 143.0 (C-3''), 146.0 (C-2′), 148.5 (C-4), 150.2 (C-6), 174.8 (C-SH). Analytical calcd for $C_{22}H_{18}O_3S_1$ (%): C: 67.68%; H: 4.65%; N: 7.17%. Found: C: 67.32%; H: 4.29%; N: 6.80%.

4.2.3.7. 4-(3-(benzyloxy)-4-methoxyphenyl)-6-(furan-2-yl) pyrimidin-2-amine, ***4Bi****.*

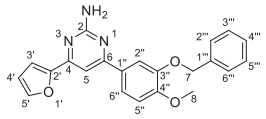

Yield: 50.20%. Light brown powder, m.p: 140–145 °C, FT-IR (cm^{-1}): 3324 and 3190 (N-H stretching), 2939 and 2840 (asymmetrical and symmetrical Csp^3-H stretching), 1646 (C = N stretching), 1599 (aromatic C = C stretching), 1513 (C = C stretching), 1266 (C-N stretching), 1177 (aromatic C-O stretching), 1019 (C-O stretching). ^1H NMR (500 MHz, DMSO d_6) δ, ppm: 2.51 (s, 3H, H-6), 5.19 (s, 2H, H-7), 6.70 (d, 1H, J = 12.0 Hz, H-5''), 7.11 (d, 1H, J = 8.5 Hz, H-6''), 7.27 (s, 2H, NH_2), 7.36–7.84 (m, 8H, H-3′,4′,5′,2'',4'', 4''',5''',6'''), 7.92 (s, 1H, H-5). ^{13}C NMR (125 MHz, DMSO d_6) δ, ppm: 56.1 (C-8), 70.6 (C-7), 99.7 (C-5), 111.8 (C-3′), 112.2 (C-2''), 122.2 (C-5''), 112.8 (C-4′), 120.8 (C-6''), 128.4 (C-2'''), 128.5 (C-4'''), 128.9 (C-3'''), 129.9 (C-1''), 137.4 (C-1'''), 145.5 (C-5′), 148.2 (C-3''), 151.8 (C-4''), 152.6 (C-2′), 156.7 (C-2), 164.1 (C-6), 164.7 (C-4). CHN elemental analysis: Calculated for $C_{22}H_{19}N_3O_3$: C: 70.76%, H: 5.13%, N: 11.25%; Found: C: 70.49%, H: 4.83%, N: 10.95%.

4.2.3.8. 4-(3-(benzyloxy)-4-methoxyphenyl)-6-(furan-2-yl) pyrimidine-2-thiol, ***4Bii****.*

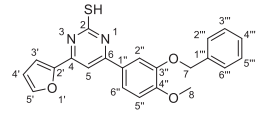

A mixture of chalcone **1** (0.01 mol) with thiourea and sodium hydroxide pellet (5 pieces) in 25 mL ethanol was refluxed for 24 h. The procedure is as mentioned in Section 3.4.3.

Yield: 26.86%. Dark brown powder, m.p: > 300 °C, FT-IR (cm^{-1}): 3032 2939 and 2847 (Csp^3-H), 2613 (S-H stretching), 1654 (C = N stretching), 1508 (aromatic C = C stretching), 1255 (C-N stretching), 1137 (aromatic C-O stretching), 1005 (C-O stretching). ^1H NMR (500 MHz, DMSO d_6) δ, ppm: 2.16 (s, 1H, SH), 4.0 (s, 3H, H-6), 5.29 (s, 2H, H-7), 6.81 (d, 1H, J = 11.5 Hz, H-5''), 7.22 (d, 1H, J = 8.0 Hz, H-5′), 7.38–7.94 (m, 7H, H-3′,4′,2'',6'',4''',5''',6'''), 8.03 (s, 1H, H-5). ^{13}C NMR (125 MHz, DMSO d_6) δ, ppm: 56.8 (C-8), 71.3 (C-7), 112.5 (C-5), 112.9 (C-3′), 112.9 (C-2''), 113.5 (C-5''), 121.5 (C-4′), 129.1 (C-6''), 129.2 (C-2'''), 129.5 (C-4'''), 130.6 (C-3'''), 138.1 (C-1''), 146.2 (C-1'''), 148.9 (C-5′), 152.5 (C-3''), 153.2 (C-4''), 157.3 (C-2′), 164.8 (C-4), 165.3 (C-6), 181.8 (C-2). CHN elemental analysis: Calculated for $C_{22}H_{18}$-

N_2O_3S: C: 67.68%, H: 4.65%, N: 7.17%. Found: C: 67.38%, H: 4.54%, N: 6.88%.

4.3. Materials and methods for Anti-Malaria

Compounds were tested for antimalarial activity by evaluation of the growth of malaria parasites in culture using the microtiter plate-based SYBR-Green-I.

4.3.1. Assay

The collected blood was diluted 20 × with complete RPMI 1640 and 100 μL was added to each well of a pre-dosed test plate containing chloroquine at a concentration range of 7.8–2000 ng/mL. The well that contains diluted blood (no drug) was included on each plate as a control. A culture of laboratory reference clone, 3D7, regarded as chloroquine-sensitive at an initial parasitaemia of 0.5% and haematocrit of 1.5% was also tested in parallel, as an additional control. The plates were placed in a modular incubator chamber and gassed (gas contains 92.5% N_2, 5.5% CO_2, 2% O_2). The chamber containing the culture was placed in an incubator at 37 °C for 72 h. The assay was terminated by freezing the plate at − 20 °C for at least 1 h before thawing. A 100 μL of LBS was added to each well and mixed thoroughly by gently tapping on the plate. The plate was covered with aluminum foil and incubated at room temperature in the dark for 3 h. Fluorescence was then read as usual. A second plate using the same patient sample and drugs was set up in parallel. Parasite growth in the second plate was monitored in the drug-free well from 20 h post-plating, by preparing blood smears using the cells in the drug free-wells. Once 60% of the parasites in the drug-free well have developed into schizonts the cells from each well were harvested onto a microscope slide. The smears were air-dried, stained with 10% Giemsa for 30 min and examined with the microscope under oil immersion. The *P. falciparum* schizonts in each smear were counted against 200 leucocytes. The concentration of anti-malarial drug inhibiting parasite growth by 50% (IC_{50}) for each drug was estimated from a dose–response curve by non-linear regression analysis using an online program, previously described by Le Nagard and Kaddouri (Kaddouri et al., 2006; Le Nagard et al., 2011). For the SG assay, fluorescence intensity was plotted against drug concentration, parasite count was plotted against drug concentration in the microscopy assay.

4.4. Molecular docking

The X-ray crystal structure of the PfATP4 receptor was downloaded from the RCSB database (PDB ID: 2DQS) (Gondokesumo et al., 2021). Biovia Discovery Studio Visualizer 16.1 was utilized to remove the heteroatoms, water, and to prepare the protein further. Eleven synthesized compounds were used as ligands in the docking studies. The 2D chemical structures of all the ligands were built using PerkinElmer ChemDraw software 16.0 and the sketched ligands were then subjected to energy minimization (MM2 force field) using PerkinElmer Chem3D 16.0 and saved in PDB format.

AutoDock 4.2 is a computational software used to prepare the ligands and protein and to generate the docking process (Rizvi et al., 2013). A click-by-click protocol was used to enforce this process (Rizvi et al., 2013). Initially, the polar hydrogens and Kollman charges were added to the PfATP4 receptor. Then, the selected ligands were revitalized by Gasteiger charges. The grid box's size was set to 70*70*70, and the coordinates were 39.3479, −2.4636, 123.9359 (as x, y, z, respectively) with a spacing of 0.375. The PfATP4 receptor was defined as rigid for the docking parameter while all ligands were flexible. The genetics algorithm run was set to 100, and the Lamarckian genetic was selected to proceed with the docking, while the remaining parameters were kept as default. Docking scores were interpreted using Discovery Studio Visualizer 16.1, so that the ionic bonds, hydrogen bonds, and hydrophobic interactions could be easily observed (Forli et al., 2016).

Declaration of Competing Interest

The authors declare that they have no known competing financial interests or personal relationships that could have appeared to influence the work reported in this paper.

Acknowledgment

The authors would like to thank Universiti Sains Malaysia for the facilities and Kementerian Pengajian Tinggi, Malaysia for the FRGS-2019 grant (203.PKIMIA.6711789) that was used to financially support this work.

References

Baer, K., Klotz, C., Kappe, S.H., Schnieder, T., Frevert, U., 2007. Release of hepatic Plasmodium yoelii merozoites into the pulmonary microvasculature. PLoS Pathog. 3, (11) e171.

Batagin-Neto, A., Lavarda, F.C., 2014. The correlation between electronic structure and antimalarial activity of alkoxylated and hydroxylated chalcones. Med. Chem. Res. 23 (2), 580–586.

Bennani, F.E., Doudach, L., Cherrah, Y., Ramli, Y., Karrouchi, K., Ansar, M., Faouzi, M.E.A., 2020. Overview of recent developments of pyrazole derivatives as an anticancer agent in different cell line. Bioorg Chem. 97,. https://doi.org/10.1016/j.bioorg.2019.103470 103470.

Bouwman, S.A., Zoleko-Manego, R., Renner, K.C., Schmitt, E.K., Mombo-Ngoma, G., Grobusch, M.P., 2020. The early preclinical and clinical development of cipargamin (KAE609), a novel antimalarial compound. Travel Med. Infect. Dis. 36,. https://doi.org/10.1016/j.tmaid.2020.101765 101765.

Cama, J., Henney, A.M., Winterhalter, M., 2019. Breaching the Barrier: Quantifying Antibiotic Permeability across Gram-negative Bacterial Membranes. J. Mol. Biol. 431 (18), 3531–3546. https://doi.org/10.1016/j.jmb.2019.03.031.

Cheo, S.W., Khoo, T.T., Tan, Y.A., Yeoh, W.C., Low, Q.J., 2020. A case of severe Plasmodium knowlesi malaria in a post-splenectomy patient. Med. J. Malaysia 75 (4), 447–449.

Forli, S., Huey, R., Pique, M.E., Sanner, M.F., Goodsell, D.S., Olson, A.J., 2016. Computational protein–ligand docking and virtual drug screening with the AutoDock suite. Nature Protocols 11 (5), 905–919.

Gondokesumo, M.E., Putra, G.S., Suhud, F., Sulistyowaty, M.I., 2021. In-silico Studies and Synthesis of 1, 3-benzoxazine Derivatives as Antimalarial Agent through PfATP4 Receptor Inhibition. Int. J. Pharm. Res. 12 (2).

Gupta, T., Rohilla, A., Pathak, A., Akhtar, M.J., Haider, M.R., Yar, M.S., 2018. Current perspectives on quinazolines with potent biological activities: A review. Synthetic Commun.. 48 (10), 1099–1127.

Hameed, A., Masood, S., Hameed, A., Ahmed, E., Sharif, A., Abdullah, M.I., 2019. Anti-malarial, cytotoxicity and molecular docking studies of quinolinyl chalcones as potential anti-malarial agent. J. Computer-aided Mol. Des. 33 (7), 677–688.

Haston, J.C., Hwang, J. and Tan, K.R., 2019. Guidance for Using Tafenoquine for Prevention and Antirelapse Therapy for Malaria - United States, 2019. MMWR Morbidity and mortality weekly report. 68(46), 1062-1068. https://doi.org/10.15585/mmwr.mm6846a4.

Ibrahim, M.M., 2015. Synthesis and characterization of new 3, 5-disubstituted-4, 5-dihydro-1H-pyrazole and their carbothioamide derivatives. European J. Chem. 6 (1), 78–83.

Ibrahim, M.M., Al-Refai, M., Abu El-Halawa, R., 2012. Synthesis of Some New Chalcone and 4, 5-Dihydro-1H-Pyrazole Derivatives as Potential Antimicrobial Agents. Jordan J. Chem. 146 (611), 1–9.

Insuasty, B., Montoya, A., Becerra, D., Quiroga, J., Abonia, R., Robledo, S., Vélez, I.D., Upegui, Y., Nogueras, M., Cobo, J., 2013. Synthesis of novel analogs of 2-pyrazoline obtained from [(7-chloroquinolin-4-yl) amino] chalcones and hydrazine as potential antitumor and antimalarial agents. European J. Med. Chem. 67, 252–262.

Insuasty, B., Ramírez, J., Becerra, D., Echeverry, C., Quiroga, J., Abonia, R., Robledo, S.M., Vélez, I.D., Upegui, Y., Munoz, J.A., 2015. An efficient synthesis of new caffeine-based chalcones, pyrazolines and pyrazolo [3, 4-b][1, 4] diazepines as potential antimalarial, antitrypanosomal and antileishmanial agents. European J. Med. Chem. 93, 401–413.

Jain, K.S., Arya, N., Inamdar, N.N., Auti, P.B., Unawane, S.A., Puranik, H.H., Sanap, M.S., Inamke, A.D., Mahale, V.J., Prajapati, C.S., Shishoo, C.J., 2016. The Chemistry and Bio-Medicinal Significance of Pyrimidines & Condensed Pyrimidines. Current Topics Med. Chem. 16 (28), 3133–3174. https://doi.org/10.2174/1568026616666160609100410.

Jampilek, J., 2017. Design of antimalarial agents based on natural products. Current Org. Chem. 21 (18), 1824–1846.

Kaddouri, H., Nakache, S., Houzé, S., Le Bras, J., 2006. Assessment of the drug susceptibility of Plasmodium falciparum clinical isolates from Africa by using a Plasmodium lactate dehydrogenase immunodetection assay and an inhibitory maximum effect model for precise measurement of the 50-percent inhibitory concentration. Antimicrobial Agents Chemother. 50 (10), 3343–3349.

Le Nagard, H., Vincent, C., Mentré, F., Le Bras, J., 2011. Online analysis of in vitro resistance to antimalarial drugs through nonlinear regression. Computer Methods Programs Biomed. 104 (1), 10–18.

Nehra, B., Rulhania, S., Jaswal, S., Kumar, B., Singh, G., Monga, V., 2020. Recent advancements in the development of bioactive pyrazoline derivatives. Eur. J. Med. Chem. 205,. https://doi.org/10.1016/j.ejmech.2020.112666 112666.

Alidmat, M.M. (2015). Synthesis and Biological Activity of New 4,6-(Diheteroaromatic)pyrimidine-2-amines. Master thesis, *Al al-Bayt University*.

Nisa, S. and Yusuf, M. (2020). Synthesis and antimicrobial evaluation of varied ring new heterocycles.

Organization, W.H. (2020). World malaria report 2020: 20 years of global progress and challenges.

Prashar, H., Chawla, A., Sharma, A.K., Kharb, R., 2012. Chalcone as a versatile moiety for diverse pharmacological activities. Int. J. Pharm. Sci. Res. 3 (7), 1913.

Qin, H.-L., Zhang, Z.-W., Lekkala, R., Alsulami, H., Rakesh, K., 2020. Chalcone hybrids as privileged scaffolds in antimalarial drug discovery: a key review. European J. Med. Chem. 193, 112215.

Rizvi, S.M.D., Shakil, S., Haneef, M., 2013. A simple click by click protocol to perform docking: AutoDock 4.2 made easy for non-bioinformaticians. Excli J. 12, 831.

Salum, K.A., Alidmat, M.M., Khairulddean, M., Kamal, N.N.S.N. M., Muhammad, M., 2020. Design, synthesis, characterization, and cytotoxicity activity evaluation of mono-chalcones and new pyrazolines derivatives. J. Appl. Pharm. Sci. 10 (08), 020–036.

Shibeshi, M.A., Kifle, Z.D., Atnafie, S.A., 2020. Antimalarial drug resistance and novel targets for antimalarial drug discovery. Infect. Drug Resistance. 13, 4047.

Sinha, S., Batovska, D.I., Medhi, B., Radotra, B., Bhalla, A., Markova, N., Sehgal, R., 2019. In vitro anti-malarial efficacy of chalcones: cytotoxicity profile, mechanism of action and their effect on erythrocytes. Malaria J. 18 (1), 1–11.

Sinha, S., Medhi, B., Sehgal, R., 2013. Chalcones as an emerging lead molecule for antimalarial therapy: a review. J. Mod. Med. Chem. 1, 64–77.

Spillman, N.J., Allen, R.J., McNamara, C.W., Yeung, B.K., Winzeler, E.A., Diagana, T.T., Kirk, K., 2013. Na(+) regulation in the malaria parasite Plasmodium falciparum involves the cation ATPase PfATP4 and is a target of the spiroindolone antimalarials. Cell host & microbe. 13 (2), 227–237. https://doi.org/10.1016/j.chom.2012.12.006.

Spillman, N.J., Kirk, K., 2015. The malaria parasite cation ATPase PfATP4 and its role in the mechanism of action of a new arsenal of antimalarial drugs. Int. J. Parasitol. Drugs Drug Resistance 5 (3), 149–162. https://doi.org/10.1016/j.ijpddr.2015.07.001.

Stewart, A.M., Grass, M.E., Brodeur, T.J., Goodwin, A.K., Morgen, M.M., Friesen, D.T., Vodak, D.T., 2017. Impact of Drug-Rich Colloids of Itraconazole and HPMCAS on Membrane Flux in Vitro and Oral Bioavailability in Rats. Mol. Pharm. 14 (7), 2437–2449. https://doi.org/10.1021/acs.molpharmaceut.7b00338.

Syahri, J., Yuanita, E., Nurohmah, B.A., Armunanto, R., Purwono, B., 2017. Chalcone analogue as potent anti-malarial compounds against Plasmodium falciparum: Synthesis, biological evaluation, and docking simulation study. Asian Pacific J. Tropical Biomed. 7 (8), 675–679.

Tadigoppula, N., Korthikunta, V., Gupta, S., Kancharla, P., Khaliq, T., Soni, A., Srivastava, R.K., Srivastava, K., Puri, S.K., Raju, K. S., Wahajuddin, Sijwali, P.S., Kumar, V. and Mohammad, I.S. (2013). Synthesis and insight into the structure-activity relationships of chalcones as antimalarial agents. J Med Chem. 56(1), 31-45. https://doi.org/10.1021/jm300588j.

Tajuddeen, N., Isah, M.B., Suleiman, M.A., van Heerden, F.R., Ibrahim, M.A., 2018. The chemotherapeutic potential of chalcones against leishmaniases: a review. Int. J. Antimicrobial Agents 51 (3), 311–318. https://doi.org/10.1016/j.ijantimicag.2017.06.010.

Tajuddeen, N., Van Heerden, F.R., 2019. Antiplasmodial natural products: an update. Malaria J. 18 (1), 1–62.

Thillainayagam, M., Pandian, L., Murugan, K.K., Vijayaparthasarathi, V., Sundaramoorthy, S., Anbarasu, A., Ramaiah, S., 2015. In silico analysis reveals the anti-malarial potential of quinolinyl chalcone derivatives. J. Biomol. Struct. Dynamics 33 (5), 961–977.

Wang, X., Chen, D., Yu, S., Zhang, Z., Wang, Y., Qi, X., Fu, W., Xie, Z., Ye, F., 2016. Synthesis and Evaluation of Biological and Antitumor Activities of Tetrahydrobenzothieno[2,3-d]Pyrimidine Derivatives as Novel Inhibitors of FGFR1. Chem. Biol. Drug. Des. 87 (4), 499–507. https://doi.org/10.1111/cbdd.12687.

Wells, T.N., 2011. Natural products as starting points for future anti-malarial therapies: going back to our roots? Malaria J. 10 (1), 1–12.

Yadav, N., Dixit, S.K., Bhattacharya, A., Mishra, L.C., Sharma, M., Awasthi, S.K., Bhasin, V.K., 2012. Antimalarial activity of newly synthesized chalcone derivatives in vitro. Chem. Biol. Drug Des. 80 (2), 340–347. https://doi.org/10.1111/j.1747-0285.2012.01383.x.

Ye, F., Wang, Y., Nian, S., Wang, Y., Chen, D., Yu, S., Wang, S., 2015. Synthesis and evaluation of biological and antitumor activities of 5,7-dimethyl- oxazolo[5,4-d]pyrimidine-4,6(5H,7H)-dione derivatives as novel inhibitors of FGFR1. J. Enzyme Inhib. Med. Chem. 30 (6), 961–966. https://doi.org/10.3109/14756366.2014.1002401.

Zhang, M.-Q., Wilkinson, B., 2007. Drug discovery beyond the 'rule-of-five'. Current Opin. Biotechnol. 18 (6), 478–488.